

The Effective Field Theory Approach to Gravitation

A Thesis

submitted to
Indian Institute of Science Education and Research Pune
in partial fulfillment of the requirements for the
BS-MS Dual Degree Programme

by

Raj Patil



Indian Institute of Science Education and Research Pune
Dr. Homi Bhabha Road,
Pashan, Pune 411008, INDIA.

April, 2020

Supervisor: Dr. Suneeta Vardarajan

© Raj Patil 2020

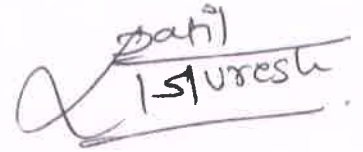
All rights reserved

Certificate

This is to certify that this dissertation entitled 'The Effective Field Theory Approach to Gravitation' towards the partial fulfilment of the BS-MS dual degree programme at the Indian Institute of Science Education and Research, Pune represents study/work carried out by Raj Patil at Indian Institute of Science Education and Research under the supervision of Dr. Suneeta Vardarajan, Associate Professor, Department of Physics, during the academic year 2019-2020.



Dr. Suneeta Vardarajan



Raj Patil

Committee:

Dr. Suneeta Vardarajan

Dr. Alok Laddha

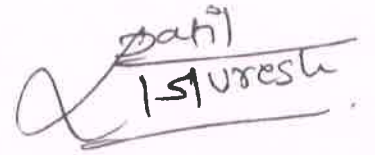
This thesis is dedicated to my parents,
who considered my education their highest priority.

Declaration

I hereby declare that the matter embodied in the report entitled 'The Effective Field Theory Approach to Gravitation', are the results of the work carried out by me at the Department of Physics, Indian Institute of Science Education and Research, Pune, under the supervision of Dr. Suneeta Vardarajan and the same has not been submitted elsewhere for any other degree.



Dr. Suneeta Vardarajan



Raj Patil

Acknowledgments

I wish to express my deepest gratitude to my advisor Dr. Suneeta Vardarajan for her guidance throughout the project. Her expertise, constant engagement, understanding, discipline, and affectionate attitude has added considerably to my experience. Special thanks to Dr. Alok Laddha for agreeing to be a member of my thesis advisory committee. I am grateful for the support provided by the INSPIRE Scholarship for Higher Education, Government of India.

I would also like to thank Prof. Sunil Mukhi for the course on Advanced Quantum Field Theory. This course has allowed me to appreciate the simplicity and beauty of quantum field theories and physics in general. I am also thankful for all the insightful discussions I had with Palash Singh and Rahul Poddar.

I would also like to thank Abhishek, Anvesha, Arindam, Niramay, Palash, Prasham, Prasanna, Rahul, Shivani, Shomik, and Sreelakshmi for all the coffee breaks, debates, stupid jokes and all the other things that made this a memorable journey.

Lastly, I would like to thank all those who believe in the open-source movement and share their work/comments/criticism extensively on the internet and promote the culture of a collective scientific voyage.

Abstract

In the light of the recent gravitational wave detections made by the LIGO and Virgo collaboration [1, 2], we study the Non-Relativistic formulation of General Relativity (NRGR) given in [3] with its extension to spinning compact objects given in [4]. Then we extend the NRGR formalism to incorporate the effects of electromagnetic charge on the constituents of the binary. We incorporate the photon field in NRGR by giving the field decomposition and power counting rules. Using these, we develop the Feynman rules to describe photon and graviton interactions with point particle worldline. We then find the corrections to the Einstein-Infeld-Hoffmann Lagrangian [5] due to the presence of the photon field and electromagnetic charge on the constituents of the binary.

Contents

- Abstract** **xi**

- Introduction** **1**

- 1 Preliminaries** **5**
 - 1.1 Notations and Conventions 5
 - 1.2 Effective Field Theories 6
 - 1.3 General Relativity 7

- 2 Compact Objects** **11**
 - 2.1 Point Particle Action 11
 - 2.2 Internal Structure 12
 - 2.3 Matching 14

- 3 Non-Relativistic General Relativity** **17**
 - 3.1 Length Scales 17
 - 3.2 Field Decomposition 18
 - 3.3 Conservative Dynamics 19
 - 3.4 Calculating Potential 23
 - 3.5 Effacement Theorem 24
 - 3.6 Dissipative Dynamics 25
 - 3.7 Multipole EFT 28
 - 3.8 Calculating Waveform 33
 - 3.9 Calculating Power 34
 - 3.10 Radiation Reaction 35
 - 3.11 Dissipative Effects 38
 - 3.12 Higher-order Corrections 39

| | | |
|----------|--|-----------|
| 4 | Spinning Compact Objects | 41 |
| 4.1 | Action for a Spinning Point Particle | 41 |
| 4.2 | Conservative Dynamics | 45 |
| 4.3 | Calculating Potential | 47 |
| 4.4 | Contribution to the Internal structure | 49 |
| 4.5 | Dissipative Dynamics | 50 |
| 4.6 | Dissipative Effects | 52 |
| 5 | Charged Compact Objects | 55 |
| 5.1 | Action for the Photon | 55 |
| 5.2 | Expansion Parameter | 56 |
| 5.3 | Field Decomposition | 56 |
| 5.4 | Conservative Dynamics | 57 |
| 5.5 | Calculating Binding Potential | 59 |
| 6 | Discussion and Conclusion | 63 |

Introduction

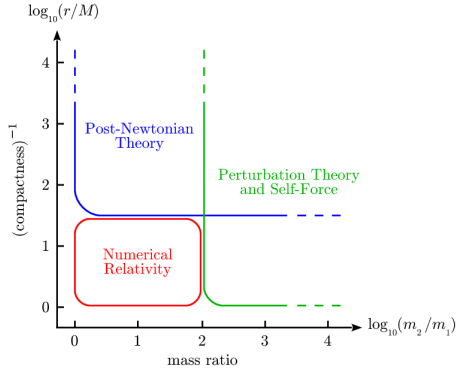
'If bliss was it in that dawn to be alive in the last twenty-five years, then, to be young in the coming decade would be the very heaven!' -Bala Iyer [6]

Gravitational waves (GW) were first predicted by Einstein in 1916 [7], where he described the propagation of gravitational waves and later in 1918 [8], he computed the energy emitted by a source i.e., the famous quadrupole formula. In 1938, Einstein with Infeld and Hoffmann calculated the first correction in orders of v^2/c^2 to the Newtonian potential due to the effects of General Relativity (GR). This allowed for determining the conservative dynamics of the objects in a given system to a certain precision. The first indirect detection of GWs was in 1974 by R. A. Hulse and J. H. Taylor [9]. They observed the period of a binary system of pulsars, which decreased due to the emission of GWs precisely as predicted by General Relativity. After around hundred years of first predicting gravitational waves, the LIGO and Virgo collaboration in 2016 [1] detected gravitational waves emitted by a black hole binary.

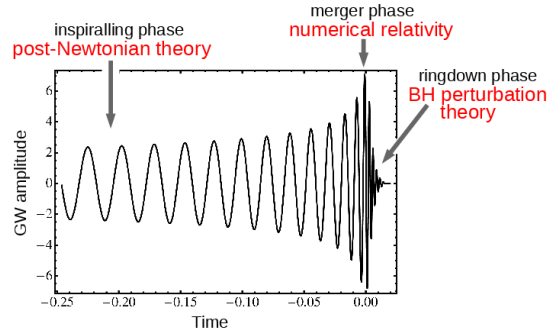
The waveform of the detected signal is a chirp - amplitude and frequency increases with time as shown in figure 1b, and can be separated into three categories:

1. Inspiral phase - where the velocities of the constituents is non-relativistic and the distance between the constituents is large as compared to the radius of the constituents. In this case, the waveform has an approximately constant frequency and not much power is emitted.
2. Merger phase - where the velocities of the constituents are relativistic and the distance between the constituents is less than the ISCO of the constituents. In this case, the waveform has rapidly increasing frequency and high amplitude because of large power emission. Here the constituents collide with each other and form single object.
3. Ringdown phase - where the final object settles down to the stable compact object like a Kerr Black Hole (BH).

Each of the above categories could be studied using different techniques as shown in figure 1a. The inspiral phase, due to its non-relativistic nature, could be analytically studied in detail using the techniques of Post-Newtonian approximation [10, 11]. Such approximations break down in the merger phase and we need to solve the full GR for two compact objects. Yet known analytical techniques cannot be used in this phase, so we used the numerical techniques [12]. The final phase of ringdown can also be studied analytically using the methods of BH perturbation theory [13, 14].



(a) Techniques used to model different phases of the waveform, where, $M = m_1 + m_2$ and r is the size of the system. Source: [15]



(b) The three phases of the coalescence of binary. Source: [16]

Figure 1

In this report, we focus on the inspiral phase. The binary system in this phase has three different length scales namely, R_s associated with the compact constituent of the binary, the radius of the orbit r and the wavelength of the emitted gravitational wave λ . The availability of multiple length scales allow us to use the techniques of Effective field theory (EFT) which exactly does the job of explaining the simplest framework that captures the essential physics at different scales. A tower of EFTs associated with inspiral phase was given by Walter Goldberger and Ira Rothstein in [3]. At first glance one should expect the EFT computations to use a lot of unnecessary tools of Quantum field theories and thus be much complicated than the classical calculations. But the usefulness of the EFTs become visible in the manifest power counting techniques that allow us to determine the relevance of the operators at the level of action i.e., we can determine ahead of any calculation the number of terms in the point particle Lagrangian that will appear at any order in the expansion parameter. Also all the divergences in the computation could be dealt with the textbook regularization and renormalization schemes.

In this tower given in figure 2, we develop an EFT around a point particle action to describe the compact object like BH and Neutron star (NS) at scales larger than the R_s . We match this EFT to the full overarching theory of BH or neutron stars to determine the unknown parameters in the EFT. The beauty of EFT approach is that, even if we aim to study the effects of the internal structure of compact objects in a bound state of binary, we can match the unknown coefficients with the overarching theory of isolated compact objects using simple computation of any relevant observable like scattering processes, rather than solving the complete problem of motion explicitly. The EFT approach manages to disentangle the highly non-linear effects general relativity when dealing with the internal structure of the compact objects in a bound state of a binary. Because we work at the level of action when using the EFT approach, we can just use two such point particle EFTs to describe a bound state like binary. In the regime of non-relativistic velocities of the

constituents, this EFT is called as Non-Relativistic General Relativity (NRGR). But this also contains some irrelevant degrees of freedom in the context of the observed waveform in the detectors. So we develop an EFT describing the multipole moments of the binary and match this to the theory of NRGR.

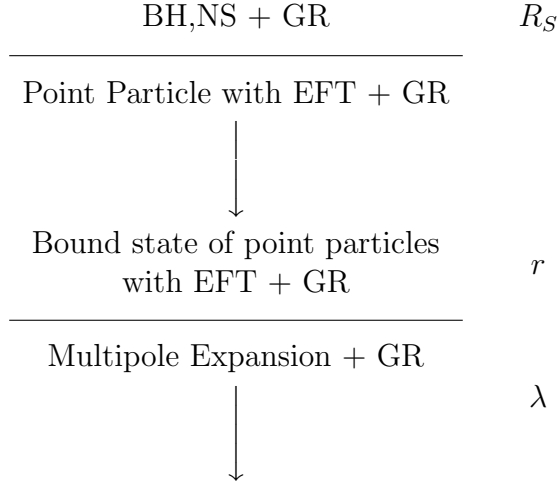


Figure 2: The tower of EFT

A general compact object like BH, NS, etc. has at least three parameters - mass, angular momentum and electromagnetic charge. The additional degrees of freedom that describe the spin of the compact objects in binary was first used in the context of NRGR in [4]. In this analysis, we aim to extend NRGR formalism to include the effects of the electromagnetic charge on the constituents of the binary on its dynamics. A similar analysis was done previously by adding a scalar field to the NRGR formalism in [17]. Here we add a photon field to the NRGR formalism and study its interactions with the other fields. Our analysis leads to a correction to the Einstein-Infeld-Hoffmann (EIH) Lagrangian at 1PN which agrees with previously done analysis in [18] in the corresponding limit of charge larger than the mass of the constituents of the binary.

The outline of this thesis is as follows. Chapter 1 has a brief introduction of the Effective Field Theories and General Relativity. In chapter 2, we develop the EFT about the point to describe the compact objects. In chapter 3, we develop the EFT that describes the dynamics of the binary in the Inspiral phase. Then we develop the multipole EFT to describe the binary at the scale of the wavelength of the emitted wave. After matching this EFT to the NRGR, we calculate the power radiated and the waveform of the emitted wave. In chapter 4, we study the effects of the spin of the binary constituents on the dynamics of the binary, power radiated and the waveform of the emitted wave. In chapter 5, we study the effects of the electromagnetic charge of the binary constituents on the dynamics of the binary.

Chapter 1

Preliminaries

In this chapter, we give a brief review of the essential techniques of Effective Field Theory (EFT) and General Relativity (GR). Readers familiar with these topics can skip to the next chapter.

1.1 Notations and Conventions

- We work in natural units where $\hbar = c = 1$ in this thesis.
- The Newton's constant G_N is written in term of the Plank's mass M_{Pl} as $G_N = 1/(32\pi M_{Pl}^2)$.
- The signature used for the metric in this thesis is mostly minus, i.e. $(1, -1, -1, -1)$.
- Partial derivatives $\partial/\partial x^\mu$ is denoted by ∂_μ and the covariant derivative is denoted by ∇_μ .
- We use the Einstein's summation notation to simplify the calculation. Greek indices run over $0, 1, 2, 3$ and the Latin indices are used for the spacial components ie $a, b, c, \dots = 1, 2, 3$.
- The three vectors are denoted by bold letters, e.g. $\mathbf{x}, \mathbf{y}, \dots$ and the unit vectors are denoted by bold letters with a hat, e.g. $\hat{\mathbf{x}}, \hat{\mathbf{y}}, \dots$
- The path integrals are denoted by the integral over the corresponding field given by

$$Z[J] = \int D\phi e^{iS[\phi, J]}$$

where the $S[\phi, J]$ is the action of the field ϕ and J is the source. If the field ϕ has a corresponding gauge transformation, the gauge fixed path integral is denoted by $D[\phi]$.

- The time averaged quantities are denoted by $\langle X(t) \rangle = \frac{1}{T} \int_0^T dt X(t)$.

1.2 Effective Field Theories

There is exciting physics at different scales in a given system. To study these different scales, either one needs to know the full overarching theory, or one needs to know the different theories corresponding to each scale. Also, one intuitively expects that the high energy theories should be irrelevant in describing the low energy phenomenon up to a certain degree of accuracy. For example, one does not need to know the details of Standard Model to determine the energy spectrum of Hydrogen atom. EFTs exactly do the job of explaining the simplest framework that captures the essential physics at different scales. These also have a mechanism to decouple the high energy physics from the effective low energy theories, i.e. we can calculate low energy observables without knowing the full overarching theory with a few unknown parameters which have to be fixed by experiments. EFTs are well suited to the problems with multiple scales, where only a few relevant degrees of freedom interact at the corresponding scales. In this section, we give a brief overview of the essential techniques of EFT needed in this thesis. A detailed overview of effective field theories could be found in [19, 20]

The two approaches to use the techniques of EFT are called the top-down approach and the bottom-up approach respectively. In the top-down approach, a high energy theory is known and one needs a low energy limit for simplicity of calculation. Whereas in the bottom-up approach, low energy theory is known and one wants to construct the effective high energy theory. One of the essential theorems used in both the approaches was given by T.Appelquist and J.Carazzone [21] which states

Theorem 1 (Decoupling theorem). *Given a renormalizable theory in which some fields have masses much larger than the others, a renormalization prescription can be found such that the heavy particles decouple from the low energy physics, except for producing renormalization effects and corrections that are suppressed by a power of the experimental momentum over a heavy mass.*

This theorem explains the concept of decoupling of high energy physics from low energy observables which is essential for the top-down approach. Consider two quantized scalar fields ϕ and Φ , whose dynamics is given by the Lagrangian

$$S = \int d^4x [(\partial_\mu \phi)^2 + m^2 \phi^2 + (\partial_\mu \Phi)^2 + M^2 \Phi^2 + \lambda \phi^2 \Phi] \quad (1.1)$$

where $M \gg m$. For calculating any physical observable at the energy scale much less than M , the field Φ decouples and could be integrated out. This procedure of integrating out a field leads to an effective action S_{EFT} given by

$$e^{iS_{EFT}[\phi]} = \int D\Phi e^{S[\phi, \Phi]} \quad (1.2)$$

and the effects of the integrated field are seen in the couplings of the S_{EFT} .¹ One can easily show that integrating a field to decouple it is equivalent to writing an effective Lagrangian

¹The integration of a field Φ produces non-local terms in Lagrangian, which could be converted to an

using the theorem 2 valid upto energy scales M and then matching the coefficients of the effective theory to the full theory such that all the physical observables are equal in both the theories.² Another important theorem was given by Steven Weinberg [22] which states

Theorem 2 (Weinberg theorem). *To any given order in perturbation theory, and for a given set of asymptotic states, the most general Lagrangian containing all terms allowed by the assumed symmetries will yield the most general S -matrix elements consistent with analyticity, perturbative unitarity, cluster decomposition and assumed symmetries.*

This theorem explains the construction of an effective theory if the high energy theory is unknown to us. This construction requires the relevant degrees of freedom and the symmetries of the system and leads us to the effective Lagrangian with infinite set of unknown coefficients called as Wilson coefficients. These have to be determined by experiments or by matching to an overarching theory. But identifying such infinite number Wilson coefficients is unphysical and one needs an expansion parameter to evaluate the importance of different terms in the effective Lagrangian. Using such a Lagrangian, we can compute the low energy observables to desired precision in orders of the expansion parameter.

1.3 General Relativity

General Relativity is the theory of gravity where a four-dimensional manifold describes the spacetime. The dynamics of the spacetime is governed by the matter distribution on it and the dynamics of the matter by the underlying spacetime. This is given by the field equation for gravity, also known as Einstein's equation. We here describe the techniques of quantum field theory used for describing the gravity namely, the propagators and vertices for graviton - the particle that carries the force of gravity. A detail overview about the general theory of relativity could found in [23, 24, 25].

1.3.1 Action for gravity

In the General theory of relativity, the effects of gravity are encoded in the structure of the underlying manifold and its dynamics. The dynamical degrees of freedom for this are the metric components $g_{\mu\nu}(x)$. For these metric components to be dynamical, we construct the action for its dynamics using the field strength tensor $R_{\mu\nu\alpha\beta}(x)$ known as the Riemann tensor. We also demand this theory to be invariant under general coordinate transformation so that physics in different frame of references remain the same. Using the theorem by Weinberg

infinite number of local terms using the techniques of operator product expansion followed by Taylor expansion.

²The procedure of matching is similar to the renormalization group equations. Matching is the flow of coefficients across the energy scale M , where the theories have different particle content above and below the scale M . Whereas, the renormalization group equation is the result of the matching of two theories with the same particle content across energy μ and $\mu + d\mu$.

and the assumed symmetries of the theory, we can write the most general Lagrangian as

$$S_{grav} = \int d^4x \sqrt{-g} (c_0 + c_1 R + c_2 R^2 + c_3 R_{\mu\nu} R^{\mu\nu} + \dots) \quad (1.3)$$

where the first term represents the cosmological constant $c_0 = \Lambda$, the second term is known as Einstein-Hilbert action with $c_1 = M_{Pl}^2$ and so on. In this thesis, we only focus on the Einstein-Hilbert action and neglect the effects of the cosmological constant and all the higher order terms.

The dynamics of the matter present in the gravitational system is given by the action S_M , which includes the corresponding matter fields. Together with the gravity part, the total action is given by

$$S = M_{Pl}^2 \int d^4x \sqrt{-g} R + S_M \quad (1.4)$$

where the M_{Pl}^2 is the coupling between the matter part and the gravity part of the action. The equation of motion derived from the above action are known as Einstein's field equations and are given by

$$R_{\mu\nu} - \frac{1}{2} R g_{\mu\nu} = 8\pi G_N T_{\mu\nu} \quad (1.5)$$

where the $T_{\mu\nu}$ is known as the energy-momentum tensor given by

$$T^{\mu\nu} = \frac{-2}{\sqrt{-g}} \frac{\delta S_M}{\delta g_{\mu\nu}}. \quad (1.6)$$

Some solutions to the above equation in the absence of the matter fields are Minkowski metric ($\eta_{\mu\nu}$), which describes the flat spacetime, Schwarzschild metric, which describes any spherically symmetric object and Kerr spacetime, which describes any axially symmetric object.

1.3.2 Semi-classical gravity

In this subsection, we study the perturbation of the metric around a particular classical solution. In foresight, we choose this classical solution to be the flat spacetime $\eta_{\mu\nu}$. Then the metric could be decomposed as,

$$g_{\mu\nu} = \eta_{\mu\nu} + \frac{h_{\mu\nu}}{M_{pl}} \quad (1.7)$$

where, $|h_{\mu\nu}/M_{pl}| \ll 1$ and factors of M_{pl} are used appropriately to normalize the kinetic term. We will then quantize the perturbation $h_{\mu\nu}$ to get a spin 2 field representing a graviton. The dynamics of the quantized perturbations are calculated using the path integral

$$Z[\Phi] = \int Dh_{\mu\nu} e^{iS_{EH}[\eta_{\mu\nu} + h_{\mu\nu}/M_{pl}] + iS_M[\Phi, \eta_{\mu\nu} + h_{\mu\nu}/M_{pl}]} \quad (1.8)$$

where the field Φ constitutes of all the matter fields present in the system. The above given action is invariant under general coordinate transformation given by $x^\mu \rightarrow x^\mu + \xi^\mu$. This

Fourier space in a simplified way as

$$\frac{h_{\mu\nu}(k)}{M_{pl}} = -\frac{i}{2M_{pl}^2} P^{\mu\nu\alpha\beta} \frac{i}{k^2 + i\epsilon} \mathcal{T}^{\alpha\beta}(k) \quad (1.14)$$

where $\mathcal{T}^{\alpha\beta}$ is called the pseudo stress-energy tensor. This could also be taken to be the definition of $\mathcal{T}^{\alpha\beta}$ in Fourier space to all orders of $h_{\mu\nu}$. The pseudo stress-energy tensor $\mathcal{T}^{\alpha\beta}$, gets the contribution from all the terms in the Lagrangian except the kinetic term which produces the left-hand side in the above equation. The $\mathcal{T}^{\alpha\beta}$ acts like a source of a single graviton and could be computed using the Feynman diagrams corresponding to one point functions of the graviton.

Chapter 2

Compact Objects

A lot of objects like black holes, neutron stars, etc. could be approximated as point particles at low energies, when seen from far away. In this chapter, we describe the relativistic point particle action and its interaction with gravitons. Then using the principles of Effective field theories (EFT), we discuss the procedure to add the description of the internal structure of such a compact object to the action for point particles. We use the bottom-up approach to describe the effective dynamics of the compact object when analyzed from far away. Then we perform an explicit matching to determine the Wilson coefficients. The EFT constructed in this chapter is then used in the next to describe a binary made up of two such compact objects.

2.1 Point Particle Action

The motion of a point particle on an arbitrary spacetime is described by the geodesics of the underlying manifold in the theory of general relativity. This description ignores the back reaction of the point particle on the underlying manifold.¹ The action for a relativistic point particle in arbitrary background $g_{\mu\nu}$ is given by,

$$\begin{aligned} S_{pp} &= -m \int ds \\ &= -m \int d\lambda \sqrt{g_{\mu\nu} \frac{dx^\mu}{d\lambda} \frac{dx^\nu}{d\lambda}} d^4x \delta^4(x^\mu - x_{pp}^\mu(\lambda)) \end{aligned} \quad (2.1)$$

where $x_{pp}^\mu(s)$ is the trajectory of the particle. The worldline of the point particle is denoted by a solid line in the Feynman diagrams in this thesis. The energy-momentum tensor corresponding to the above action is given by

$$T_{pp}^{\mu\nu} = m \int d\lambda \frac{u^\mu u^\nu}{\sqrt{u^2}} \frac{\delta^4(x^\mu - x_{pp}^\mu(\lambda))}{\sqrt{-g}} \quad (2.2)$$

where, the $u^\mu = dx^\mu/d\lambda$ is the four-velocity of the point particles and for stationary particles, it could be taken as $v^\mu = (1, \mathbf{0})$ and $\sqrt{u^2}$ in the denominator is to make the $T_{pp}^{\mu\nu}$ re-parametrization invariant.

¹More details about the backreaction of a point particle on the underlying manifold could be found in [26].

2.2 Internal Structure

Now we have successfully described the theory of point particle in the arbitrary background and the field produced by them. We are now interested in the description of the internal degrees of the freedom associated with an object approximated as a point particle. We are interested in studying the object with an associated length scale R_S like a black hole, a neutron star, etc. because this scale allows us to make the following separation. As we are only interested in the effects of the object at long-distance, we break the metric corresponding to these compact objects in short-distance modes $g_{\mu\nu}^S$ with the associated length scale less than or of the order of R_S , and long-distance modes $g_{\mu\nu}^L$ whose associated length is larger than R_S . The separation is denoted as

$$g_{\mu\nu} = g_{\mu\nu}^S + g_{\mu\nu}^L \quad (2.3)$$

Now to get an effective theory at long-distance, we integrated out the short-distance modes and the internal degrees of freedom of the object. We then get

$$e^{iS_{EH}[g_{\mu\nu}^L] + iS_{EFT}[x_{(cm)}(\sigma), g_{\mu\nu}^L]} = \int D[g_{\mu\nu}^S] D\delta x_n(\lambda_n) e^{iS_{EH}[g_{\mu\nu}] + iS_{int}[x_n(\lambda_n), g_{\mu\nu}^S]} \quad (2.4)$$

where $x_n(\lambda_n)$ are the internal degrees of freedom of the object, S_{int} describes their interaction with the short-range field and the S_{EFT} is the effective theory at large distance that describes the effective degrees of freedom $x_{(cm)}(\sigma)$ the compact object. This S_{EFT} will be valid in the regime of $\omega R_S \ll 1$, where ω is the energy corresponding to the experiment and R_S is the length scale corresponding to the compact object. In the example of a neutron star, $x_n(\lambda_n)$ represents the position of $10^{40} m^{-3}$ constituent particles and $x_{(cm)}(\sigma)$ represents the center of mass of the star. Now the details about the structure of the object are encoded in the coefficients of the effective Lagrangian.

The computation of the integral over the short-distance modes and the internal degrees of freedom of the object is very difficult. For example, in the case of a neutron star, S_{int} is the interaction of each particle in the star with the short-distance modes and is usually unknown to us. So rather than computing the integral, we construct an EFT for the S_{EFT} . For the construction, we use the symmetries of diffeomorphism invariance (gauge invariance) and re-parametrization invariance of the worldline of the effective point particle at long-distance. The simplest term that we can write in the Lagrangian following all the assumed symmetries is the Lagrangian given in equation (2.1) that dictates the dynamics of a point particle i.e., the center of mass of the compact object. The only other way to make a gauge invariant term is using the Riemann tensor, its contractions with the metric or the four-velocity $u^\alpha(\lambda)$ corresponding to the effective degrees of freedom of the object. The Riemann tensor then can be written in terms of Ricci tensor and Weyl tensor. The contractions of Ricci tensor (and Ricci scalar) with the four-velocities could be removed using field redefinition $g_{\mu\nu} \rightarrow g_{\mu\nu} + \delta g_{\mu\nu}$ [3], which leads to the following change in the S_{EH} ,

$$\delta S_{EH} = M_{pl}^2 \int d^4x \sqrt{-g} \left(R_{\mu\nu} - \frac{1}{2} \eta_{\mu\nu} R \right) \delta g^{\mu\nu} . \quad (2.5)$$

The contraction of Weyl tensor with $u^\alpha(\sigma)$ could be written in the term of $E_{\mu\nu} = C_{\mu\alpha\nu\beta}u^\alpha u^\beta$ and $B_{\mu\nu} = \frac{1}{2}\epsilon_{\mu\alpha\beta\sigma}C_{\nu\rho}^{\alpha\beta}u^\sigma u^\rho$. Due to the antisymmetry property of $E_{\mu\nu}$ and $B_{\mu\nu}$ we could have only terms of the form $(E_{\mu\nu})^n$, $(B_{\mu\nu})^n$ and contractions of their derivatives like $u^\alpha\nabla_\alpha E_{\mu\nu}$ and $u^\alpha\nabla_\alpha B_{\mu\nu}$.

The internal structure of the compact object are encoded in the multipole moments of the compact object given by $Q_{abc\dots k}$. The total multipole moments of the object can be separated as

$$Q_{abc\dots k} = \langle Q_{abc\dots k} \rangle_S + \langle Q_{abc\dots k} \rangle_R \quad (2.6)$$

where $\langle Q_{abc\dots k} \rangle_S$ is the inherent internal structure of the isolated compact object obtained after integrating over the short-distance modes $g_{\mu\nu}^S$. The $\langle Q_{abc\dots k} \rangle_R$ is then the response of the internal structure of the compact object to the long-distance modes $g_{\mu\nu}^L$. This response is considered to be a small perturbation in the region where the EFT is valid ($\omega R_S \ll 1$) and thus are studied as quantize excitations about the classical background of inherent internal multipole moments. Because the excitations are small, we also assume the dependence of the multipole moments on the source is linear with correctly imposed causality.

For example, let's consider the leading order contribution of multipole moments given by the quadrupole moment to the point particle. The simplest term that could be added to the effective action using the quadrupole moment and the allowed functions of the long-distance metric is given by

$$S_{Q(E)} = \frac{1}{2} \int d\tau d^4x \delta^4(x - x(\tau)) Q_{(E)}^{ij}(\tau) E_{ij}(x). \quad (2.7)$$

Now we assume that the compact object we are interested in is spherically symmetric and thus the $\langle Q_{ab} \rangle_S$ and all higher-order internal multipole moments are zero. To simplify the calculations further, we assume the response of the multipole moments depends linearly on the incident gravitational waves. Thus the response quadrupole moments are given by

$$\langle Q_{ab} \rangle_R(\tau) = \frac{1}{2} \int d\tau' d^4x \delta^4(x - x(\tau')) G_{abij}^{ret}(\tau, \tau') E_{ij}(x) \quad (2.8)$$

where the retarded Green's function is given by

$$G_{abij}^{ret}(\tau, \tau') = \langle [Q_R^{ab}(\tau), Q_R^{ij}(\tau')] \rangle \theta(\tau - \tau'). \quad (2.9)$$

To ensure the causality of the response, we choose the retarded propagator. In the frequency domain, the quadrupole propagator can be written using the spherical symmetry of the object as

$$iG_{abij}^{ret}(\omega) = Q_{abij} F(\omega) \quad (2.10)$$

where, $Q_{abij} = \delta_{ai}\delta_{bj} + \delta_{aj}\delta_{bi} - (2/3)\delta_{ab}\delta_{ij}$. Using the techniques of linear response theory one can easily see that the real part of $G_{abij}^{ret}(\omega)$ is even function of ω and thus describes the conservative contributions from the internal structure whereas, the imaginary part of $G_{abij}^{ret}(\omega)$ is odd function of ω and thus describes the dissipative contributions from the internal structure. This could be easily generalized to the magnetic type and higher-order multipole moments.

To obtain the conservative sector of the effective Lagrangian, the real part of the function $F(\omega)$ can then be expanded in powers of ω as

$$\text{Re}[F(\omega)] = C_E + C_{\dot{E}}\omega^2 + \dots \quad (2.11)$$

The conservative effective action could be then written using the symmetries of the long-distance scale and the conservative contribution from the internal structure of the compact objects as

$$\begin{aligned} S_{eff}[x_{(cm)}(\sigma), g_{\mu\nu}^L] = & \int d^4x d\sigma \delta^4(x - x_{xm}(\sigma)) \left[-m \sqrt{g_{\mu\nu}^L(x) u_{(cm)}^\mu(\sigma) u_{(cm)}^\nu(\sigma)} \right. \\ & + c_E E_{\mu\nu}(x) E^{\mu\nu}(x) + c_{\dot{E}} u^\alpha(\sigma) \nabla_\alpha E_{\mu\nu}(x) u^\beta(\sigma) \nabla_\beta E^{\mu\nu}(x) + \dots \\ & \left. + c_B B_{\mu\nu}(x) B^{\mu\nu}(x) + c_{\dot{B}} u^\alpha(\sigma) \nabla_\alpha B_{\mu\nu}(x) u^\beta(\sigma) \nabla_\beta B^{\mu\nu}(x) + \dots \right] \quad (2.12) \end{aligned}$$

where the first term is the Lagrangian for a point particle and the other terms make up the conservative effective action due to the internal structure of the compact object. Terms with higher power of $E_{\mu\nu}$ and $B_{\mu\nu}$ could be obtained by implementing the above given method on higher-order multipole moments. The unknown coefficients called the Wilson coefficients have to be fixed by either matching this EFT to an overarching theory or by doing experiments.

2.3 Matching

In this section, we match the effective theory to the full general theory of relativity and find the scaling of the unknown Wilson coefficients of the conservative effective theory and the unknown function $\text{Im}[F(\omega)]$. For this, We match the graviton scattering cross-section computed by both the theories.

First, we consider the conservative sector and compute the following diagram using the effective theory given in equation (2.12). The result corresponds to

$$\begin{array}{c} \overline{C_E} \\ \text{wavy line} \\ h_{ab}(t, \mathbf{k}) \quad h_{ij}(t, \mathbf{k}) \end{array} \approx \frac{\omega^4 C_E}{M_{pl}^2} \quad (2.13)$$

One can easily show that this is the only diagram in the conservative sector, proportional to the fourth power of ω . Thus the total graviton scattering cross-section calculated using the EFT of point particles with internal structure is given by

$$\sigma_{EFT}^{(sca)}(\omega) = \dots + \frac{C_{E(B)}^2 \omega^8}{M_{pl}^4} + \dots \quad (2.14)$$

In the case of classical General Relativity (GR), a spherically symmetric object (Schwarzschild spacetime) has only one length scale - Schwarzschild radius associated with it. In the region

where the EFT is valid, namely $\omega R_S \ll 1$, we can expand the gravitational wave scattering cross-section as [27]

$$\sigma_{GR}^{(sca)}(\omega) = R_s^2 f(R_s\omega) \approx R_s^2 (\dots + (R_s\omega)^8 + \dots) \quad (2.15)$$

where the function f is analytic and is expanded in the power series of $R_s\omega$, which only shows us the scaling behavior of the cross-section. Matching the above given two results we obtain

$$C_E \approx M_{pl}^2 R_s^5 \quad (2.16)$$

upto some numerical factors. This result is universal for any spherically symmetric object, but to find the exact result of a particular object, one has to perform the exact matching. For Schwarzschild black hole, the Wilson coefficients $C_{E(B)}$ vanish [28], whereas, for neutron stars they are finite and related to 'Love numbers' [29]. Now following a similar procedure, it is very easy to calculate the Wilson coefficients corresponding to the higher-order multipole moments. Using the tools of power counting developed in the next chapter, we can find the importance of all effective operators in the conservative sector.

In the case of the dissipative sector, we have to calculate the absorption cross-section of gravitons in the Fock space of response multipole moments. For this, we consider the following diagrams,

$$\begin{array}{c} \overline{Q_{ij(R)}} \\ \text{wavy line} \\ h_{ab}(t, \mathbf{k}) \end{array} = \frac{i}{8M_{pl}^2} \int d\tau e^{-i\omega\tau} \left(\omega^2 \epsilon_{ij}^* \epsilon_{ab} \langle Q_{ab}^{(E)}(0) Q_{ij}^{(E)}(\tau) \rangle \right. \\ \left. + (\mathbf{k} \times \epsilon^*)_{ij} (\mathbf{k} \times \epsilon)_{ab} \langle Q_{ab}^{(B)}(0) Q_{ij}^{(B)}(\tau) \rangle \right) \quad (2.17)$$

The imaginary part of the above diagram represents the absorption cross-section of gravitons and is obtained by using the cutting rules given in in chapter 8 of [43]. The cutting rules make the propagator of the response quadrupole moment on-shell and leads to

$$\sigma_{EFT}^{(abs)}(\omega) = \frac{\omega^3}{2M_{pl}^2} \text{Im} [F(\omega)] \quad (2.18)$$

In the case of GR, the absorption cross-section for a spherically symmetric Schwarzschild spacetime [30] in the regime $\omega R_S \ll 1$ is given by

$$\sigma_{GR}^{(abs)}(\omega) = \frac{4\pi}{45} R_S^6 \omega^4 \quad (2.19)$$

Matching the above given two results we obtain

$$\text{Im} [F(\omega)] = \frac{16}{45} G_N^5 m^6 \omega \quad (2.20)$$

The above result is exact for a Schwarzschild black hole and one has to perform the matching independently for a different object like neutron star using the graviton absorption cross-section in the corresponding metric. The calculation of absorption cross-section from EFT and classical GR could be extended to the higher power of ω and thus, the matching result could also be extended to have higher odd powers of ω . The $\text{Im}[F(\omega)]$ could be substituted

back in the propagator of the multipole moments to obtain an effective action for the dissipative sector like the one for conservative sector given in equation (2.12). But it is easier to interpret the Feynman diagrams in terms of multipole moments for the dissipative sector so that the role of cutting rules become easier to understand. The effects of the dissipative sector are further analyzed in the section 3.11 of the next chapter.

Chapter 3

Non-Relativistic General Relativity

Once we know how to incorporate the internal structure of the object, we move on towards the description of a binary system in General Relativity (GR). In this chapter, we describe the Effective Field Theory (EFT) way of classical Post-Newtonian (PN) expansion called the Non-Relativistic General Relativity (NRGR) developed by Walter Goldberger and Ira Rothstein in [3]. We first decompose the field $h_{\mu\nu}$ in short-distance and long-distance modes. Then we describe the essential power counting and Feynman rules necessary to integrate over short-distance modes. Then we calculate the binding potential at 1PN that describes the conservative dynamics of the binary. To describe the radiation emitted to infinity by the binary, we propose an EFT of multipole moments. Then we match this EFT to the theory with the internal structure of the binary and calculate the moments. Using the multipole moments we then calculate the power radiated by the binary. One expects that the radius of the binary will shrink due to the back-reaction of the radiated power. To incorporate this effect in our description, we introduce the In-In formalism and then calculate the leading order back reaction. We conclude the section by depicting the higher-order non-linear corrections.

3.1 Length Scales

With only one object in the picture, we only have one length scale R_s associated with it. But in the bound state of two point particles, we have new length scales, namely the radius of the orbit r and the wavelength of the emitted gravitational wave λ . If we assume the velocities of the particles to be slow, then we have a hierarchy of length scales

$$\lambda \gg r \gg R_s \tag{3.1}$$

where R_s is the length scale of the internal structure of the object in the binary. The leading order behavior of the system is governed by a $1/r$ Newtonian interaction. Then the velocity relates the size of the objects to the radius of the binary and is also the ratio of the emitted wavelength and the radius of the binary given by

$$v^2 \approx \frac{G_N m}{r} \approx \frac{R_s}{r} \quad \text{and} \quad v \approx \frac{r}{\lambda} \tag{3.2}$$

respectively. So it makes v/c a good candidate as for the expansion parameter. Another small parameter at hand is \hbar/L , where L is the angular momentum of the binary. We use

v/c as the primary expansion parameter where the n^{th} order in v^2/c^2 is called as the n^{th} in the Post-Newtonian expansion (nPN) in the language of classical gravity and use \hbar/L to suppress the quantum effects (loop diagrams).

3.2 Field Decomposition

Here we assume that the particles move on a flat background $\eta_{\mu\nu}$ and thus the effects of binary are seen as perturbation $h_{\mu\nu}$ to it. So we can decompose the metric as

$$g_{\mu\nu} = \eta_{\mu\nu} + \frac{h_{\mu\nu}}{M_{pl}} . \quad (3.3)$$

The description of the dynamics of binary is obtained after integrating over the perturbation that encodes the internal structure of the binary. The effective action S_{EFT} is then given by

$$e^{iS_{EFT}[x_{pp}^{(a)}(\sigma_a)]} = \int D[h_{\mu\nu}] e^{iS_{EH}[g_{\mu\nu}] + iS_{int}[x_{pp}^{(a)}(\sigma_a), g_{\mu\nu}]} . \quad (3.4)$$

where, $x_{pp}^{(a)}(\sigma_a)$ is the position of the a^{th} point particle in the binary. As we are only interested in the long-distance physics at the scales of λ , we first break the field in short-distance modes - potential gravitons $H_{\mu\nu}$ and long-distance modes - radiation gravitons $\bar{h}_{\mu\nu}$ as

$$h_{\mu\nu} = H_{\mu\nu} + \bar{h}_{\mu\nu} \quad (3.5)$$

and then integrate out the short-distance modes to get an effective long-distance theory. This decomposition is done by identifying the modes by their scaling with respect to v and r . The long-distance modes represent the emitted on-shell gravitons and scale as

$$(k_0, \mathbf{k}) \approx \left(\frac{v}{r}, \frac{v}{r} \right) \quad (3.6)$$

because k_0 is like the frequency of the graviton and should scale like the inverse of period of the binary given by r/v and so does \mathbf{k} . On the other hand, the short-distance modes are off-shell and scale as

$$(k_0, \mathbf{k}) \approx \left(\frac{v}{r}, \frac{1}{r} \right) \quad (3.7)$$

because the wave vector \mathbf{k} has the dimensions of the inverse length and the only parameter at this scale is the distance between the particles in the binary $1/r$. This decomposition was first proposed by Walter Goldberger and Ira Rothstein in [3].¹

Due to the decomposition given in the equation (3.5), we can break the integration over the perturbation shown in equation (3.4) in two steps. First to describe the effective dynamics of the point particles, we construct an EFT with a systematic non-relativistic expansion in v/c obtained after integrating out the short-distance modes. The effective

¹Such decomposition is motivated by the techniques of ‘Method of Regions’ developed for loop integrals in [31, 32].

action is given by

$$e^{iS_{NRGR}[x_{pp}^{(a)}(\sigma_a), \bar{h}_{\mu\nu}]} = \int D[H_{\mu\nu}] e^{iS_{EH}[g_{\mu\nu}] + iS_{int}[x_{pp}^{(a)}(\sigma_a), g_{\mu\nu}]} \quad (3.8)$$

where the S_{NRGR} contains the effective binding potential for point particles and the interaction of point particles with the radiation gravitons, which is responsible for the gravitational wave emission and power loss. The internal structure of the point particles R_s is described by the coefficients in S_{int} given by equation (2.12) and the internal structure of the binary r is governed by the potential gravitons. In the next section, we compute the path integral over the potential modes and the second integral over the radiation graviton will be considered in later sections.

3.3 Conservative Dynamics

For calculating the binding potential of the binary, we only consider the dynamics of the potential modes and its interactions with point particles. For $\bar{h}_{\mu\nu} = 0$ in the NRGR action, the dynamics of the binary becomes conservative and the effective action $W_{EFT}[x_p]$ describing it is given by

$$e^{iW_{EFT}[x_{pp}^{(a)}]} = \int D[H_{\mu\nu}] e^{iS_{EH}[H_{\mu\nu}] + iS_{int}[x_{pp}^{(a)}(\sigma_a), H_{\mu\nu}]} \quad (3.9)$$

where $S_{EH}[H_{\mu\nu}]$ describes the dynamics and self-interaction of the potential graviton and the S_{int} given by equation (2.12) describes the dynamics of a point particle with internal structure and its interaction with potential gravitons.²

In this section, we describe the technique of power counting and give all the essential Feynman rules for propagators and vertices. Using these Feynman rules, we aim to calculate the first correction to the binding potential at 1PN called the Einstein-Infeld-Hoffmann Lagrangian in the next section. The effects of the radiation gravitons make the dynamics non-conservative and are studied in the section 3.6.

3.3.1 Propagators

We first look at the $S_{EH}[H_{\mu\nu}]$, where the quadratic term in the field given in equation (1.10) gives us the propagator given in equation (1.11) and the higher-order terms give us the nonlinear graviton self-interaction vertices. Due to small velocities of the point particles, the propagator could be expanded in series as

$$\frac{1}{k^2} \approx \frac{-1}{\mathbf{k}^2} \left[1 + \frac{k_0^2}{\mathbf{k}^2} + \frac{k_0^4}{\mathbf{k}^4} + \dots \right]. \quad (3.10)$$

²Note that the back-reaction on the point particles due to its interaction with a single potential graviton is of the order of $|k|/|p| \approx 1/L \ll 1$, so, the point particles are treated as background non-dynamical sources for computing the dynamics in the conservative sector.

So the momentum space Feynman rule for the propagator of the potential graviton is

$$H_{\mu\nu}(t_1, \mathbf{p}) \overset{\text{-----}}{\overrightarrow{\mathbf{p}}} H_{\alpha\beta}(t_2, \mathbf{p}) \equiv \frac{-iP_{\mu\nu\alpha\beta}}{\mathbf{k}^2} \delta(t_1 - t_2) \quad (3.11)$$

and higher-orders of k_0^2/\mathbf{k}^2 are taken into account by propagator correction given by equation (3.16).

3.3.2 Power counting

To arrange the terms in the Lagrangian in increasing order of expansion parameter, we need to have a manifest power counting in v . For this, we need to know the scaling behavior of the field and its derivatives. At the leading order, the propagator for potential modes scale as

$$\langle H_{\mu\nu}(x) H_{\alpha\beta}(y) \rangle \approx \int dk_0 d^3\bar{\mathbf{k}} \frac{1}{\mathbf{k}^2} e^{ik(x-y)} \approx \frac{v}{r^2} \quad (3.12)$$

and so the potential gravitons scales as

$$H_{\mu\nu}(x) \approx \frac{\sqrt{v}}{r}. \quad (3.13)$$

The scaling of its derivatives could be identified by using the Fourier transform of the graviton and is given by

$$\partial_0 H_{\mu\nu}(x) \approx \frac{v}{r} H_{\mu\nu}(x) \quad \text{and} \quad \partial_i H_{\mu\nu}(x) \approx \frac{1}{r} H_{\mu\nu}(x). \quad (3.14)$$

The velocity of the particles in the orbit depends on the strength of the gravitational coupling constant M_{pl} . So M_{pl} also scales as $1/\sqrt{Lv}$. It will be convenient to have the scaling behavior of $H_{\mu\nu}/M_{pl}$ and is given by

$$\frac{H_{\mu\nu}(x)}{M_{pl}} \approx \frac{v^2}{\sqrt{L}}. \quad (3.15)$$

Using the above given scaling of the graviton field, its derivatives, the scaling of k_0 and \mathbf{k} and the scaling of M_{pl} , we can figure out the scaling of all possible terms added in the effective action. For a Feynman diagram, the propagators do not scale but the vertices do, and their scaling is decided by the corresponding term in the Lagrangian.

3.3.3 Vertices

The vertices in the Lagrangian given in equation (3.9) have three kind of interaction vertices: ones which are generated by the correction to the propagator due to the expansion, ones which are generated by the cubic and higher-order terms in $S_{EH}[H_{\mu\nu}]$ and the ones due to the EFT constructed for S_{int} .

For the first kind of vertices, the scaling of the corrections to the propagator given in equation (3.10) is given by $k_0^2/\mathbf{k}^2 \approx v^2$. We define momentum space Feynman rule for a two-point interaction vertex as,

$$H_{\mu\nu}(t_1, \mathbf{p}_1) \text{---} \overset{v^2}{\otimes} \text{---} H_{\alpha\beta}(t_2, \mathbf{p}_2) \quad \equiv \quad \int dt \delta^3\left(\sum_{k=1}^2 \mathbf{p}_k\right) \left(\partial_{t_1} \partial_{t_2}\right) \quad (3.16)$$

to reproduce the propagator at higher-orders in v^2 . higher-orders of correction could be obtained by attaching multiple vertices, each producing a factor of k_0^2/\mathbf{k}^2 in the propagator.

For the second kind, the scaling of the cubic term in the $S_{EH}[H_{\mu\nu}]$ is of the form

$$\frac{1}{M_{pl}} \int dt d^3\mathbf{x} H^2 \partial^2 H \approx \frac{v^2}{\sqrt{L}}. \quad (3.17)$$

This term could be represented by the three-point graviton vertex given by the Feynman rule

$$\begin{array}{c} \text{---} \\ | \\ \text{---} \end{array} \quad v^2/\sqrt{L} \quad \text{given in equation (A.33) of [33]} \quad (3.18)$$

So adding a loop of potential gravitons to any diagram adds a factor of v^4/L . All the higher-order terms in $H_{\mu\nu}$ will have an extra factor of M_{pl} in the denominator and thus scale with the higher power of v . We here aim to calculate the binding potential up to order v^2 and all the diagrams having higher point self-interaction graviton vertices contribute to higher-order in v^2 . So, all such terms are S_{EH} ignored for now.

For the third kind, the leading term in the Lagrangian given in (2.12) could be expanded as

$$\begin{aligned} - \sum_{a=1,2} m_a \int ds \sqrt{g_{\mu\nu}} \frac{dx^\mu}{ds} \frac{dx^\nu}{ds} d^4x \delta^4(x^\mu - x_a^\mu(s)) = \\ - \sum_{a=1,2} m_a \int dt \left[1 - \frac{1}{2} \mathbf{v}^2 + \frac{1}{2} \frac{H_{00}}{M_{pl}} + \frac{H_{0i}}{M_{pl}} \mathbf{v}^i + \frac{1}{2} \frac{H_{ij}}{M_{pl}} \mathbf{v}^i \mathbf{v}^j \right. \\ \left. - \frac{1}{8} \mathbf{v}^4 + \frac{1}{4} \frac{H_{00}}{M_{pl}} \mathbf{v}^2 + \frac{1}{8} \left(\frac{H_{00}}{M_{pl}} \right)^2 + \dots \right]. \quad (3.19) \end{aligned}$$

The scaling of terms independent of the graviton field representing the kinetic energy and corrections to it is given by

$$\int dt m \mathbf{v}^2 \approx L ; \quad \int dt m \mathbf{v}^4 \approx Lv^2 \quad \text{and so on.} \quad (3.20)$$

These terms do not contain $H_{\mu\nu}$ and thus do not contribute to Feynman diagrams and are carried over to the $W_{eff}[x_p]$. The scaling of the linear term in field coupling it with the point

particle is given by

$$\int dt \frac{H_{00}}{M_{pl}} \approx \sqrt{L}; \quad \int dt u^i \frac{H_{i0}}{M_{pl}} \approx \sqrt{L}v; \quad \int dt u^2 \frac{H_{00}}{M_{pl}} \approx \sqrt{L}v^2 \quad \text{and} \quad \int dt u^i u^j \frac{H_{ij}}{M_{pl}} \approx \sqrt{L}v^2. \quad (3.21)$$

The corresponding Feynman rules are given by

$$\begin{array}{c} \sqrt{L} \\ \hline x_a(t) \\ \vdots \downarrow \mathbf{p} \\ H_{00}(t, \mathbf{p}) \end{array} \equiv - \sum_{a=1,2} \frac{im_a}{2M_{pl}} \int dt e^{i\mathbf{p} \cdot \mathbf{x}_a(t)}; \quad (3.22)$$

$$\begin{array}{c} \sqrt{L}v \\ \hline x_a(t) \\ \vdots \downarrow \mathbf{p} \\ H_{0i}(t, \mathbf{p}) \end{array} \equiv - \sum_{a=1,2} \frac{im_a}{M_{pl}} \int dt \mathbf{v}_a^i e^{i\mathbf{p} \cdot \mathbf{x}_a(t)} \quad \text{and} \quad (3.23)$$

$$\begin{array}{c} \sqrt{L}v^2 \\ \hline x_a(t) \\ \vdots \downarrow \mathbf{p} \\ H_{ij}(t, \mathbf{p}) \end{array} + \begin{array}{c} \sqrt{L}v^2 \\ \hline x_a(t) \\ \vdots \downarrow \mathbf{p} \\ H_{00}(t, \mathbf{p}) \end{array} \equiv - \sum_{a=1,2} \left[\frac{im_a}{2M_{pl}} \int dt \mathbf{v}_a^i \mathbf{v}_a^j e^{i\mathbf{p} \cdot \mathbf{x}_a(t)} + \frac{im_a}{4M_{pl}} \int dt v_a^2 e^{i\mathbf{p} \cdot \mathbf{x}_a(t)} \right]. \quad (3.24)$$

The scaling of the leading quadratic term in field coupling it with the point particle is given by

$$\int dt \frac{H_{00}}{M_{pl}} \frac{H_{00}}{M_{pl}} \approx v^2 \quad (3.25)$$

which corresponds to the following Feynman rule

$$\begin{array}{c} v^2 \\ \hline x_a(t) \\ \swarrow \downarrow \mathbf{q} \quad \downarrow \mathbf{p} \\ H_{00}(t, \mathbf{q}) \quad H_{00}(t, \mathbf{p}) \end{array} \equiv - \sum_{a=1,2} \frac{im_a}{8M_{pl}} \int dt e^{i\mathbf{p} \cdot \mathbf{x}_a(t)} e^{i\mathbf{q} \cdot \mathbf{x}_a(t)}. \quad (3.26)$$

Similarly, terms which contribute to a higher-order of v are ignored. In all the above vertices, if the vertex contains free index, then it has to be contracted with the same free index in the corresponding propagator for example, vertex with \mathbf{v}^i or $\mathbf{v}^i \mathbf{v}^j$ has to be contracted with $P_{i0\cdots}$ or $P_{ij\cdots}$ respectively. And if a vertex does not have a free index, then it should be contracted with $P_{00\cdots}$.

3.4 Calculating Potential

In this section, we explicitly calculate the first few terms of the Lagrangian for the action given in equation (3.9). We have obtained this action by integrating out potential gravitons and ignoring the radiation ones. This corresponds to the contributing diagrams having the property that they are connected after removing the worldlines of the particles, internal lines correspond to potential gravitons and we do not have external on-shell potential gravitons. We ignore all the diagrams that contain graviton loops because adding a loop adds a factor of v^4/L to the diagrams and makes it suppressed by a huge factor of $1/L$. We also ignore all the diagrams with graviton self-energy terms which could be made zero by the techniques of dimensional regularization.

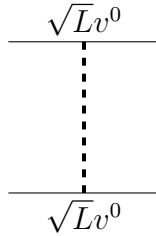


Figure 3.1: This diagram contributes at order Lv^0 to the effective action in equation (3.9).

Then at order Lv^0 we have the diagram given in figure 3.1. This could be computed using the result in equation (B.3) of [33]. The corresponding Lagrangian is given by

$$L_N = \sum_{a=1,2} \frac{1}{2} m_a \mathbf{v}_a^2 + \frac{G_N m_1 m_2}{|\mathbf{r}|} \quad (3.27)$$

where the first term represents the kinetic energy of the particle, the second is the Newtonian gravitational potential with $G_N = 1/(32\pi M_{pl}^2)$ being the Newton's constant.

At order Lv^1 , we have only one diagram made from the vertex in equation (3.23) and (3.22). The contribution of such diagram go to zero due to the identity $P_{i000} = 0$.

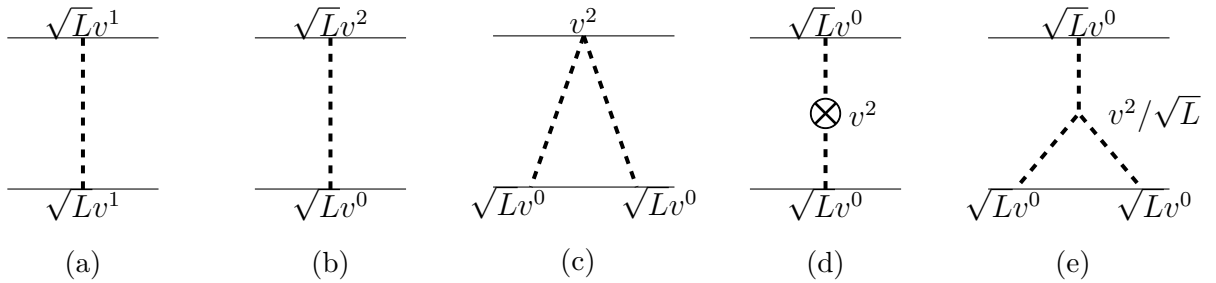


Figure 3.2: These diagrams contribute at order Lv^2 to the effective action in equation (3.9).

At order Lv^2 we have the diagrams given in figure 3.2. The diagrams in figure 3.2a, 3.2b and 3.2c are straight forward to compute using the result in equation (B.3) of [33]. For the diagram in figure 3.2d, we use the equation (B.4) of [33] and for the diagram in figure 3.2e, we use the equations (B.3) and (A.34) in [33]. The results then correspond to the following Lagrangian

$$L_{EIH} = \sum_{a=1,2} \frac{1}{8} m_a \mathbf{v}_a^4 + \frac{G_N m_1 m_2}{2|\mathbf{r}|} \left[3(\mathbf{v}_1^2 + \mathbf{v}_2^2) - 7(\mathbf{v}_1 \cdot \mathbf{v}_2) - \frac{(\mathbf{v}_1 \cdot \mathbf{r})(\mathbf{v}_2 \cdot \mathbf{r})}{\mathbf{r}^2} \right] - \frac{G_N^2 m_1 m_2 (m_1 + m_2)}{2\mathbf{r}^2} \quad (3.28)$$

called as the Einstein-Infeld-Hoffmann Lagrangian. The original derivation of this result can be found in [3] in the context of NRGR, and agrees with the previously derived results by A. Einstein, L. Infeld and B. Hoffmann in 1938 [5]. The equation of motion of the binary constituents could be found by applying the Euler-Lagrange equations to the above Lagrangian.

The higher-order terms could be found by using the techniques of temporal Kaluza-Klein parametrization of the metric suggested by Kol and Smolkin in [34]. This simplifies the three and higher point interaction vertices by replacing them with simple vertices but more in number. The 2PN and higher order calculations could be found in [35, 36, 37]. The public package EFTofPNG [38], which was created for highprecision computation in the EFT of PN Gravity, could also be used to carry the higher PN calculations.

3.5 Effacement Theorem

In this section, we analyze the effects of the internal structure of the compact object on their dynamics in the binary system. Using the result of matching done in section 2.3, the Wilson coefficient corresponding to response quadrupole moment of the conservative sector scales as

$$C_{E(B)} \approx M_{pl}^2 R_s^5. \quad (3.29)$$

Once we have the relationship between the $C_{E(B)}$ and the R_s , we now compute the scaling of the term with $C_{E(B)}$ as its coefficient as

$$\frac{C_E}{M_{pl}^2} \int (\partial_i \partial_j H_{00})^2 dt \approx v^{10} \quad (3.30)$$

where we have used the virial theorem to get $H_{00}/M_{pl} \approx G_N/r$. Following the matching procedure given in the section 2.3, one can easily find that this is the leading order contribution of the conservative sector of the internal structure of the compact object to the effective point particle Lagrangian in the PN expansion.

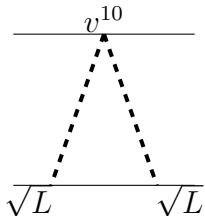


Figure 3.3: This diagram corresponds to the leading contribution of the conservative internal structure of the compact objects that contributes to the conservative dynamics at order Lv^{10} .

The vertex given in equation (3.30) contributes first to the effective action by the diagram given in figure 3.3 at order Lv^{10} . Thus the internal structure of the compact objects corresponding to the conservative sector response, first contributes to the dynamics of the binary at 5PN. This also supports the assumption of taking objects like black holes and neutron stars to be point particles at first few orders.

3.6 Dissipative Dynamics

Once we have calculated the conservative dynamics by computing the integration over the potential gravitons given in equation (3.4), we move on to the second integral over the radiation graviton in this section. After integrating out the potential graviton, we are left with the action

$$S_{NRGR}[\mathbf{x}_a, \bar{h}_{\mu\nu}] = W_{EFT}[\mathbf{x}_a] + S_1[\mathbf{x}_a, \bar{h}_{\mu\nu}] + S_2[\mathbf{x}_a, \bar{h}_{\mu\nu}] + S_{NL}[\mathbf{x}_a, \bar{h}_{\mu\nu}] \quad (3.31)$$

where, W_{EFT} describes the conservative dynamics, S_1 has the linear terms in $\bar{h}_{\mu\nu}$, S_2 has the quadratic terms in $\bar{h}_{\mu\nu}$ which give us the propagator and its corrections, and S_{NL} has the nonlinear interactions between the sources and the $\bar{h}_{\mu\nu}$. In this section, we describe the propagator and power counting for the radiation graviton. We also give the Feynman rules corresponding to the terms S_1 , S_2 and S_{NL} appearing in the above action.

3.6.1 Propagators

We first look at the S_2 , which leads us to the propagator given in equation (1.12) and the higher-order terms give us the nonlinear graviton self-interaction vertices. The momentum space Feynman rule for the propagator of the radiation graviton is

$$\bar{h}_{\mu\nu}(t_1, \mathbf{p}) \text{ --- } \underset{\mathbf{p}}{\text{wavy}} \text{ --- } \bar{h}_{\alpha\beta}(t_2, \mathbf{p}) \quad \equiv \quad \frac{-iP_{\mu\nu\alpha\beta}}{k^2} . \quad (3.32)$$

Now any correction to the propagators of radiation graviton due to integration over the potential ones like loops, etc. will be down by at least a factor of \sqrt{L} and thus will be ignored in this thesis.

3.6.2 Power counting

To arrange the terms in the Lagrangian in increasing order of expansion parameter, we need to have a manifest power counting in v . For this, we need to know the scaling behavior of the field and its derivatives. At the leading order, the propagator for radiation modes scale as

$$\langle \bar{h}_{\mu\nu}(x) \bar{h}_{\alpha\beta}(y) \rangle \approx \int dk_0 d^3\mathbf{k} \frac{1}{k^2} e^{ik(x-y)} \approx \frac{v^2}{r^2} \quad (3.33)$$

and so the radiation gravitons and its derivatives scales as

$$\bar{h}_{\mu\nu}(x) \approx \frac{v}{r} \quad \text{and} \quad \partial_i \bar{h}_{\mu\nu}(x) \approx \frac{v}{r} \bar{h}_{\mu\nu}(x). \quad (3.34)$$

It will be convenient to have

$$\frac{\bar{h}_{\mu\nu}}{M_{pl}} \approx \frac{v^2 \sqrt{v}}{\sqrt{L}}. \quad (3.35)$$

Using the above given scaling of the radiation graviton, its derivatives, the scaling of k_0 and \mathbf{k} and the scaling of M_{pl} , we can figure out the scaling of all possible terms in the effective action. For a Feynman diagram, the propagators do not scale, but the vertices do, and their scaling is decided by the corresponding term in the Lagrangian.

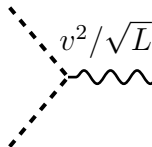
3.6.3 Vertices

The Lagrangian given in equation (3.31) has two kinds of interaction vertices: ones which are generated by the cubic and higher-order terms in $S_{EH}[H_{\mu\nu}]$ and the ones due to the EFT constructed for S_{int} .

For the first kind, the scaling of the leading cubic term of $S_{EH}[h_{\mu\nu}]$ is given by

$$\frac{1}{M_{pl}} \int dt d^3\mathbf{x} \bar{h} H \partial_i^2 H \approx \frac{v^2 \sqrt{v}}{\sqrt{L}} \quad (3.36)$$

which could be represented by the three-point graviton vertex given by the Feynman rule



given in equation (A.29) of [33].

(3.37)

Each diagram with time derivative acting on $H_{\mu\nu}$ instead of the spatial derivative, will be higher by an order of v . Every $\bar{h}_{\mu\nu}$ instead of $H_{\mu\nu}$ in the above diagram will have an extra factor of \sqrt{v} . One can easily calculate the vertices that contribute to higher-orders of v but we here aim to calculate the power radiated up to the leading orders and thus, all higher-order terms are ignored.

For the second kind, the term for the point particles contributing to the action could

be expanded as

$$\begin{aligned}
-\sum_{a=1,2} m_a \int d\tau &= -\sum_{a=1,2} m_a \int dt \left[1 - \frac{1}{2} \mathbf{v}^2 - \frac{1}{8} \mathbf{v}^4 + \frac{1}{2} \frac{H_{00}}{M_{pl}} + \frac{H_{0i}}{M_{pl}} \mathbf{v}^i + \frac{1}{2} \frac{H_{ij}}{M_{pl}} \mathbf{v}^i \mathbf{v}^j \right. \\
&\quad + \frac{1}{4} \frac{H_{00}}{M_{pl}} \mathbf{v}^2 + \frac{1}{8} \left(\frac{H_{00}}{M_{pl}} \right)^2 + \dots \\
&\quad + \frac{1}{2} \frac{\bar{h}_{00}}{M_{pl}} + \frac{\bar{h}_{0i}}{M_{pl}} \mathbf{v}^i + \frac{1}{2} \frac{\bar{h}_{ij}}{M_{pl}} \mathbf{v}^i \mathbf{v}^j + \frac{1}{4} \frac{\bar{h}_{00}}{M_{pl}} \mathbf{v}^2 \\
&\quad \left. + \frac{1}{8} \left(\frac{\bar{h}_{00}}{M_{pl}} \right)^2 + 2\bar{h}_{00} H_{00} + \dots \right] \tag{3.38}
\end{aligned}$$

where the first and second line of the above equation is already taken care of in section 5.4. Now we analyze at the third and fourth line, where we have the interaction of the radiation gravitons with the potential gravitons and the binary. The scaling of linear terms in the above action is given as

$$\int dt \frac{\bar{h}_{00}}{M_{pl}} \approx \sqrt{Lv}; \quad \int dt u^i \frac{\bar{h}_{i0}}{M_{pl}} \approx \sqrt{Lvv}; \quad \int dt u^2 \frac{\bar{h}_{00}}{M_{pl}} \approx \sqrt{Lvv^2} \quad \text{and} \quad \int dt u^i u^j \frac{\bar{h}_{ij}}{M_{pl}} \approx \sqrt{Lvv^2}. \tag{3.39}$$

This will produce the corresponding vertices with the given Feynman rules

$$\begin{aligned}
\frac{\sqrt{L}}{\text{wavy line } \downarrow \mathbf{p}} x_a(t) &\equiv -\sum_{a=1,2} \frac{im_a}{2M_{pl}} \int dt e^{i\mathbf{p}\cdot\mathbf{x}_a(t)}; \tag{3.40} \\
&H_{00}(t, \mathbf{p})
\end{aligned}$$

$$\begin{aligned}
\frac{\sqrt{Lv}}{\text{wavy line } \downarrow \mathbf{p}} x_a(t) &\equiv -\sum_{a=1,2} \frac{im_a}{M_{pl}} \int dt \mathbf{v}_a^i e^{i\mathbf{p}\cdot\mathbf{x}_a(t)} \quad \text{and} \\
&H_{0i}(t, \mathbf{p}) \tag{3.41}
\end{aligned}$$

$$\begin{aligned}
\frac{\sqrt{Lv^2}}{\text{wavy line } \downarrow \mathbf{p}} x_a(t) + \frac{\sqrt{Lv^2}}{\text{wavy line } \downarrow \mathbf{p}} x_a(t) &\equiv -\sum_{a=1,2} \left[\frac{im_a}{2M_{pl}} \int dt \mathbf{v}_a^i \mathbf{v}_a^j e^{i\mathbf{p}\cdot\mathbf{x}_a(t)} + \frac{im_a}{4M_{pl}} \int dt \mathbf{v}_a^2 e^{i\mathbf{p}\cdot\mathbf{x}_a(t)} \right]. \\
&H_{ij}(t, \mathbf{p}) \quad H_{00}(t, \mathbf{p}) \tag{3.42}
\end{aligned}$$

Similarly, the scaling of the leading quadratic term in the above action is given as

$$\int dt \frac{\bar{h}_{00} H_{00}}{M_{pl}} \approx v^2 \sqrt{v}. \tag{3.43}$$

which corresponds to the following Feynman rule

$$H_{00}(t, \mathbf{q}) \quad \bar{h}_{00}(t, \mathbf{p}) \quad \equiv \quad - \sum_{a=1,2} \frac{im_a}{8M_{pl}} \int dt e^{i\mathbf{p}\cdot\mathbf{x}_a(t)} e^{i\mathbf{q}\cdot\mathbf{x}_a(t)} . \quad (3.44)$$

The diagrams similar to above contributing at higher-order of v can be calculated easily but are ignored in this section. Diagrams with two or more radiation gravitons in the final state contribute at higher PN order and thus, vertices leading to such diagrams are ignored in this section.

In all the above vertices, if the vertex contains a free index, then it has to be contracted with the same free index in the corresponding propagator for example, vertex with \mathbf{v}^i or $\mathbf{v}^i \mathbf{v}^j$ has to be contracted with P_{i0-} or P_{ij-} respectively. And if a vertex does not have a free index, then it should be contracted with P_{00-} .

3.7 Multipole EFT

In this section, we study the effects of the source term S_1 for the radiation gravitons. This term could also be written using the pseudo stress-energy tensor defined in equation (1.6) as

$$S_1 = -\frac{1}{2M_{pl}} \int d^4x \mathcal{T}_{\mu\nu}(x) \bar{h}^{\mu\nu}(x) \quad (3.45)$$

where the $\mathcal{T}_{\mu\nu}$ may be either the standard stress-energy tensor of matter or it may be the pseudo stress-energy tensor, which includes some gravitational effects from the potential gravitons that correspond to the gravitational binding energy of the bound state.

The only observables we have is the waveform of the gravitational wave emitted to infinity and the corresponding power carried away from the binary in the form of gravitational waves. We study an EFT composed of the multipole moments of an object coupling to the radiation graviton given in [39] that encapsulates the essential degrees of freedom from S_1 in the above equation, needed to calculate the waveform and the radiated power far away from the sources. The action for the EFT is given as

$$\begin{aligned} S_{MP} = & -\frac{1}{2M_{pl}} \int dt [M\bar{h}_{00} + 2\mathbf{P}^i \bar{h}_{0i} + M\mathbf{X}^i \partial_i \bar{h}_{00} + \mathbf{L}^i \epsilon_{ijk} \partial_j \bar{h}_{0k}] \\ & + \sum_{l=2}^{\infty} \frac{1}{l!} \int dt I^{a_1 a_2 \dots a_l}(t) \partial_{a_1} \dots \partial_{a_{l-2}} E_{a_{l-1} a_l}(x) \\ & - \sum_{l=2}^{\infty} \frac{1}{(l+1)!} \int dt J^{a_1 a_2 \dots a_l}(t) \partial_{a_1} \dots \partial_{a_{l-2}} B_{a_{l-1} a_l}(x) \end{aligned} \quad (3.46)$$

where, the electric component is $E_{ij} = R_{0i0j}$ and magnetic component is $B_{ij} = (1/2)\epsilon_{imn} R_{0jmn}$.³

³Note that the expression of E_{ij} and B_{ij} are given for the rest frame of the binary where $u^\alpha = (1, 0, 0, 0)$.

This action will only encapsulate the effects of the propagator from $S_2[\mathbf{x}_a, \bar{h}_{\mu\nu}]$ and the terms linear in the radiation graviton $S_1[\mathbf{x}_a, \bar{h}_{\mu\nu}]$ from the equation (3.31). One has to write a similar action at each order of $\bar{h}_{\mu\nu}$ to consider all the terms from the equation (3.4). But one can show that these higher-order terms will be suppressed by at least a order of \sqrt{L} , thus are ignored until section 3.12.

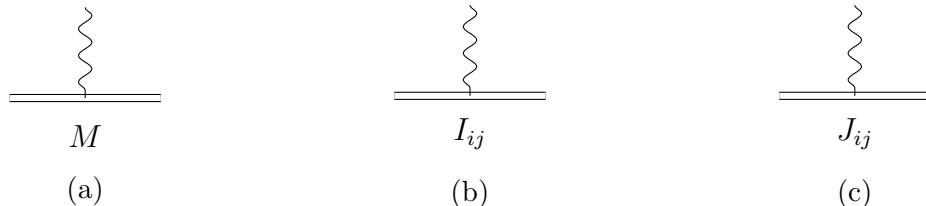


Figure 3.4: Examples of leading vertices produced by the Lagrangian given in equation (3.46).

Here the multipole moments of the object are classical and thus do not have a propagator. The worldline of the binary system is denoted by double solid lines in the Feynman diagrams of this theory. The interactions of the radiation graviton with the multipole moments are given in the vertices shown in figure 3.4, where, the distance between the double lines represents that the internal length scale of the binary is smaller than the wavelength of the emitted radiation graviton.

With the above developed techniques, we can now compute the integral over the radiation gravitons in the path integral given by

$$e^{iS_{EFT}[x_{pp}^{(a)}(\sigma_a)]} = \int D[\bar{h}_{\mu\nu}] e^{iS_{NRGR}[x_{pp}^{(a)}(\sigma_a), \bar{h}_{\mu\nu}]} . \quad (3.47)$$

The diagrams that contribute to the effective action S_{EFT} are shown in the figure 3.5. We analyze the imaginary part of these diagrams in subsection 3.9 which leads to the radiated power, and the real part in subsection 3.10 which results in the back reaction of the radiated power on the dynamics of the binary.

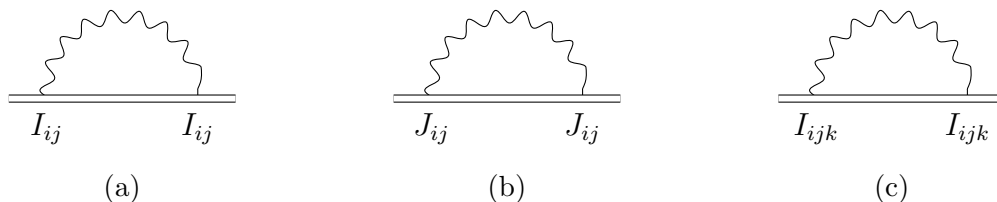


Figure 3.5: Examples of diagrams that contribute to effective action given in equation (3.47).

This will be the case in the rest of the report as we always work in the frame where $\mathbf{X} = \mathbf{P} = 0$.

3.7.1 Matching

The multipole moments are unknown in the action given in equation (3.46) and one has to match this to the action which describes the internal structure of the binary. For this, we expand the $\bar{h}(t, \mathbf{x})$ around the center of the mass of the binary to get

$$\bar{h}_{\mu\nu}(x) = \sum_{n=0}^{\infty} \frac{1}{n!} \mathbf{x}^{i_1} \cdots \mathbf{x}^{i_n} \partial_{i_1} \cdots \partial_{i_n} \bar{h}_{\mu\nu}(x^0, \mathbf{x}_{cm}). \quad (3.48)$$

Plugging the above in term S_1 of the point particle action (3.31), we get the expression for the total mass of the binary as

$$M = \int d^3x \mathcal{T}^{00}. \quad (3.49)$$

The center of mass of the binary could be written as

$$\mathbf{X}^i = \int d^3\mathbf{x} \mathcal{T}^{00} \mathbf{x}^i, \quad (3.50)$$

which could be made zero by choosing the center of the reference frame on the center of mass. The linear momentum of the binary could be identified as

$$\mathbf{P}^i = \int d^3\mathbf{x} \mathcal{T}^{0i}(x^0, \mathbf{x}) = \int d^3\mathbf{x} \dot{\mathcal{T}}^{00}(x^0, \mathbf{x}) \mathbf{x}^i \equiv m \dot{\mathbf{X}}^i, \quad (3.51)$$

which could also be made zero by going to the proper frame of the center of mass. The angular momentum is then given by

$$\mathbf{L}^i = - \int d^3\mathbf{x} \epsilon^{ijk} \mathcal{T}^{0j} \mathbf{x}^k. \quad (3.52)$$

For the higher-order multipole moments, we need to write the equation 3.45 in the irreducible representation of $S_0(3)$. This can be then compared with the EFT at long-distance and the multipole moments can be identified as [40]

$$\begin{aligned} I^{a_1 \dots a_n} = & \sum_{p=0}^{p=\infty} \left\{ \frac{(2\ell+1)!!}{(2p)!!(2\ell+2p+1)!!} \left(1 + \frac{8p(\ell+p+1)}{(\ell+1)(\ell+2)} \right) \left[\int d^3\mathbf{x} \partial_0^{2p} \mathcal{T}^{00}(t, \mathbf{x}) \mathbf{x}^{2p} \mathbf{x}^{a_1 \dots a_n} \right]_{\text{STF}} \right. \\ & + \frac{(2\ell+1)!!}{(2p)!!(2\ell+2p+1)!!} \left(1 + \frac{4p}{(\ell+1)(\ell+2)} \right) \left[\int d^3\mathbf{x} \partial_0^{2p} \mathcal{T}^{kk}(t, \mathbf{x}) \mathbf{x}^{2p} \mathbf{x}^{a_1 \dots a_n} \right]_{\text{STF}} \\ & - \frac{(2\ell+1)!!}{(2p)!!(2\ell+2p+1)!!} \left(\frac{4}{\ell+1} \right) \left(1 + \frac{2p}{(\ell+2)} \right) \left[\int d^3\mathbf{x} \partial_0^{2p+1} \mathcal{T}^{0m}(t, \mathbf{x}) \mathbf{x}^{2p} \mathbf{x}^{ma_1 \dots a_n} \right]_{\text{STF}} \\ & \left. + \frac{(2\ell+1)!!}{(2p)!!(2\ell+2p+1)!!} \left(\frac{2}{(\ell+1)(\ell+2)} \right) \left[\int d^3\mathbf{x} \partial_0^{2p+2} \mathcal{T}^{mn}(t, \mathbf{x}) \mathbf{x}^{2p} \mathbf{x}^{mna_1 \dots a_n} \right]_{\text{STF}} \right\} \end{aligned} \quad (3.53)$$

$$\begin{aligned}
J^{a_1 \dots a_n} = & \sum_{p=0}^{p=\infty} \left\{ \frac{(2\ell+1)!!}{(2p)!!(2\ell+2p+1)!!} \left(1 + \frac{2p}{(\ell+2)} \right) \left[\int d^3 \mathbf{x} \epsilon^{a_1 m n} \partial_0^{2p} \mathcal{T}^{0m}(t, \mathbf{x}) \mathbf{x}^{2p} \mathbf{x}^{na_1 \dots a_{l-1}} \right]_{\text{STF}} \right. \\
& \left. - \frac{(2\ell+1)!!}{(2p)!!(2\ell+2p+1)!!} \left(\frac{1}{(\ell+2)} \right) \left[\int d^3 \mathbf{x} \epsilon^{a_1 m r} \partial_0^{2p+1} \mathcal{T}^{mn}(t, \mathbf{x}) \mathbf{x}^{2p} \mathbf{x}^{nr a_1 \dots a_{l-1}} \right]_{\text{STF}} \right\}
\end{aligned} \tag{3.54}$$

where STF means to only consider the symmetric-tracefree part of the corresponding tensor [41]. Every time derivative of the stress-energy tensor scales like the inverse of the wavelength of the emitted radiation graviton and every \mathbf{x} scales like the radius of the binary r , where $r/\lambda \approx v$. Hence, the multipole moments scale as a series in v^2 given by $ma^l(1 + (a/\lambda) + (a/\lambda)^2 + \dots)$. Also, each higher multipole moment has a factor of $\mathbf{x}^{a_i} \partial_{a_i}$ and thus scales with a higher power of v than the previous one.

3.7.2 Calculating Multipole Moments

In this subsection, we explicitly calculate the diagrams with one graviton in the final state, which contributes to the total $T_{\mu\nu}$ using the point particle action given in equation (3.31). Then we use the above given relations between the multipole moments and the stress-energy tensor to obtain the exact expression for the moments for the first few orders in v .

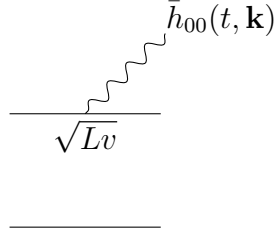


Figure 3.6: This diagram yields the $\mathcal{T}^{\mu\nu}$ at order \sqrt{Lv} .

At order \sqrt{Lv} , the diagram given in figure 3.6 leads to

$$\mathcal{T}^{00}(x^0, \mathbf{k}) = \sum_a m_a e^{-i\mathbf{k} \cdot \mathbf{x}_a} \tag{3.55}$$

Using the results from the section 3.7.1, we have

$$M = \sum_a m_a \ ; \tag{3.56}$$

$$\mathbf{X}^i = \frac{1}{M} \sum_a m_a \mathbf{x}_a^i \ ; \tag{3.57}$$

$$I^{ij} = \sum_a m_a [\mathbf{x}_a^i \mathbf{x}_a^j]^{TF} \ ; \text{ and so on.} \tag{3.58}$$

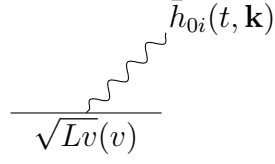


Figure 3.7: This diagram yields the $\mathcal{T}^{\mu\nu}$ at order $\sqrt{Lv}(v)$.

At order $\sqrt{Lv}(v)$, the diagram given in figure 3.7 leads to

$$\mathcal{T}^{0i}(x^0, \mathbf{k}) = \sum_a m_a \mathbf{v}_a^i e^{-i\mathbf{k}\cdot\mathbf{x}_a}, \quad (3.59)$$

Using the results from the section 3.7.1, we have

$$\mathbf{P}^i = \sum_a m_a \mathbf{v}_a^i + \mathcal{O}(v^3) ; \quad (3.60)$$

$$\mathbf{L}_i = \epsilon_{ijk} L^{jk} = \sum_a m_a (\mathbf{x}_a \times \mathbf{v}_a)^i + \mathcal{O}(v^3) ; \quad (3.61)$$

$$J^{ij} = -\frac{1}{2} \sum_a m_a ((\mathbf{v}_a \times \mathbf{x}_a)^i \mathbf{x}_a^j + (\mathbf{v}_a \times \mathbf{x}_a)^j \mathbf{x}_a^i) + \mathcal{O}(v^3) ; \text{ and so on.} \quad (3.62)$$

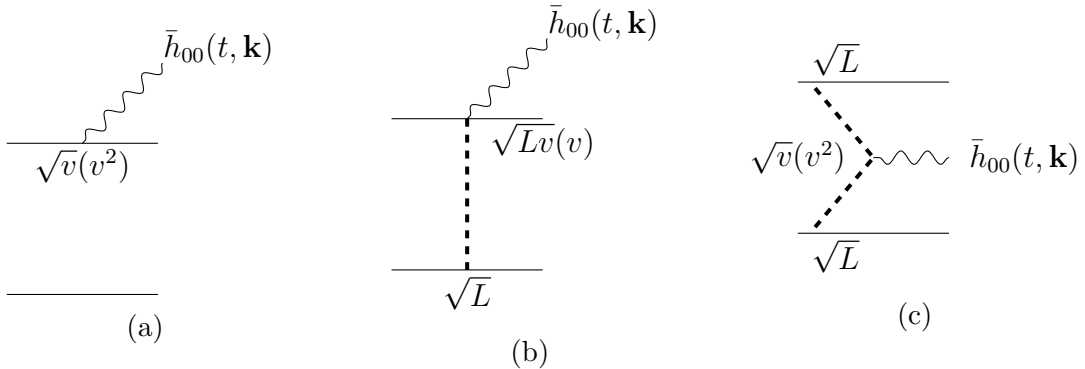


Figure 3.8: These diagrams yields the $\mathcal{T}^{\mu\nu}$ at order $\sqrt{Lv}(v^2)$.

At order $\sqrt{Lv}(v^2)$, the diagram given in figure 3.8 leads to

$$M = \sum_a m_a \left[1 + \frac{1}{2} \mathbf{v}_a^2 - \frac{1}{2} \sum_b \frac{G_N m_b}{|\mathbf{x}_a - \mathbf{x}_b|} \right] ; \quad (3.63)$$

$$\mathbf{X}^i = \frac{1}{M} \sum_a m_a \left[1 + \frac{1}{2} \mathbf{v}_a^2 - \frac{1}{2} \sum_b \frac{G_N m_b}{|\mathbf{x}_a - \mathbf{x}_b|} \right] \mathbf{x}_a^i ; \quad (3.64)$$

$$\begin{aligned} I^{ij} = & \sum_a m_a \left(1 + \frac{3}{2} \mathbf{v}_a^2 - \sum_b \frac{G_N m_b}{|\mathbf{x}_a - \mathbf{x}_b|} \right) [\mathbf{x}_a^i \mathbf{x}_a^j]^{TF} + \frac{11}{42} \sum_a m_a \frac{d^2}{dt^2} \left(\mathbf{x}_a^2 [\mathbf{x}_a^i \mathbf{x}_a^j]^{TF} \right) \\ & - \frac{4}{3} \sum_a m_a \frac{d}{dt} \left(\mathbf{x}_a \cdot \mathbf{v}_a [\mathbf{x}_a^i \mathbf{x}_a^j]^{TF} \right) ; \text{ and so on.} \end{aligned} \quad (3.65)$$

All the higher-order corrections to the multipole moments are ignored in this thesis and could be found in [39]. At order $\sqrt{Lv}(v)^n$, the first multipole moment M scales like $\sqrt{Lv}(v)^n$ and each l^{th} order moment scales like $\sqrt{Lv}(v)^{n+l}$. Using the above developed results, we calculate the emitted waveform and the power radiated in the following sections.

3.8 Calculating Waveform

In this section, we compute the waveform of the gravitational wave emitted by the binary. This waveform is computed by assuming that the detector is far away from the source and thus, we here only compute the leading order term in $1/R$, where R is the distance between the detector and the sources. We start with the retarded graviton propagator, given by

$$\langle h_{\mu\nu}(x) h_{\alpha\beta}(y) \rangle_{ret} = \frac{-i P_{\mu\nu\alpha\beta} \theta(t_x - t_y)}{4\pi |\mathbf{x} - \mathbf{y}|} \delta(t_x - t_y - |\mathbf{x} - \mathbf{y}|) \quad (3.66)$$

Using the above given propagator to invert the equation given in equation (1.14), we get

$$\begin{aligned} h_{\mu\nu}(x) = & \frac{1}{2M_{pl}} \int d^4 y \delta(\mathbf{y}) \sum_{l=2}^{\infty} \frac{1}{n!} I^{a_1 \dots a_l}(t) \partial_{a_1} \dots \partial_{a_{l-2}} \partial_{t_y} \partial_{t_y} \left[\frac{-i P_{\mu\nu a_{l-1} a_l} \theta(t_x - t_y)}{4\pi |\mathbf{x} - \mathbf{y}|} \delta(t_x - t_y - |\mathbf{x} - \mathbf{y}|) \right] \\ & - \frac{1}{2M_{pl}} \int d^4 y \delta(\mathbf{y}) \sum_{l=2}^{\infty} \frac{2l}{(l+1)!} J^{a_1 \dots a_l}(t) \partial_{a_1} \dots \partial_{a_{l-2}} \epsilon_{a_l m n} \partial_{t_y} \partial_n \left[\frac{-i P_{\mu\nu a_{l-1} m} \theta(t_x - t_y)}{4\pi |\mathbf{x} - \mathbf{y}|} \delta(t_x - t_y - |\mathbf{x} - \mathbf{y}|) \right] \end{aligned} \quad (3.67)$$

where, the spatial partial derivative acting on the $1/|\mathbf{x} - \mathbf{y}|$ leads to higher-order term in $1/R$ and thus are ignored and the spatial partial derivative acting on the delta function leads to

$$\partial_k \delta(t_x - t_y - |\mathbf{x} - \mathbf{y}|) = \partial_k(t_x - |\mathbf{x} - \mathbf{y}|) \frac{\partial \delta(t_x - t_y - |\mathbf{x} - \mathbf{y}|)}{\partial(t_x - |\mathbf{x} - \mathbf{y}|)} \quad (3.68)$$

$$= \frac{(\mathbf{x} - \mathbf{y})^k}{|\mathbf{x} - \mathbf{y}|} \frac{\partial}{\partial t_y} \delta(t_x - t_y - |\mathbf{x} - \mathbf{y}|) \quad (3.69)$$

where $(\mathbf{x} - \mathbf{y})^k / |\mathbf{x} - \mathbf{y}| = \hat{n}^k$ is the unit vector pointing towards the direction of the detector. The operator

$$\Lambda_{ijk_{l-1}k_l} = (\delta_{ik} - \hat{\mathbf{n}}_i \hat{\mathbf{n}}_k)(\delta_{jl} - \hat{\mathbf{n}}_j \hat{\mathbf{n}}_l) - \frac{1}{2}(\delta_{ij} - \hat{\mathbf{n}}_i \hat{\mathbf{n}}_j)(\delta_{kl} - \hat{\mathbf{n}}_k \hat{\mathbf{n}}_l) \quad (3.70)$$

which projects the tensor components to surface orthogonal to the unit vector n^i and then makes it transverse and trace-less. Using the identities in equation (3.68) and (3.70), we get an expression [40]

$$h_{ij}^{TT}(x) = \frac{4G}{|\mathbf{x}|} \Lambda_{ijk_{l-1}k_l} \left[\sum_{l=2}^{\infty} \frac{1}{l!} \frac{\partial^l}{\partial t^l} I^L(t_{ret}) \hat{\mathbf{n}}^{L-2} - \sum_{l=2}^{\infty} \frac{2l}{(l+1)!} \epsilon^{abk_l} \frac{\partial^l}{\partial t^l} J^{k_{l-1}bL-2}(t_{ret}) \hat{\mathbf{n}}^{aL-2} \right] \quad (3.71)$$

that describes the waveform of the wave emitted by the binary described by the EFT of multipole expansion, where $t_{ret} = t - |\mathbf{x}|$. This result matches to the known result, e.g. presented in [10].

Using the above given result and the multipole moments computed using the matching techniques given in section 3.7.1, we can compute the waveform of gravitational wave emitted by the binary.

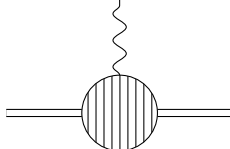
3.9 Calculating Power

In this section, we calculated the power radiated by the binary using the effective theory of multipole moments developed in the previous section. For calculating power, we use the optical theorem derived in chapter 24 of [42]. The power radiated could be written as

$$P = \int dE d\Omega E \frac{d\tau_{tot}}{dE d\Omega} = \frac{1}{T} \int dE d\Omega E \frac{d}{dE d\omega} \left[\text{Im} [S_{EFT}(x_{pp}(\sigma))] \right] \quad (3.72)$$

where E is the energy of the final state particles and the $d\tau_{tot}/dE d\Omega$ is the number of particles in that final state per unit time, energy and solid angle and this relates the total power radiated to the imaginary part of the diagram(s) contributing to the effective action. We then calculate the imaginary part of the diagrams contributing to $S_{eff}[x_{pp}^a(\lambda_a)]$ given in equation (3.47) using the cutting rules given in chapter 8 of [43].

As one can easily see, having two or more gravitons in the final state reduces the order of the diagram by at least \sqrt{L} and thus are ignored. The real part of the diagram produced by the action in equation (3.46) will give us the correction to the conservative dynamics of the binary and is discussed in section 3.10. The imaginary part of these diagrams yields the power radiated to infinity by the binary. To identify the imaginary part, we define

$$iA_h(\mathbf{k}) = \begin{array}{c} \text{---} \\ \text{---} \end{array} \text{---} \left(\text{---} \right) \text{---} \begin{array}{c} \text{---} \\ \text{---} \end{array} \quad (3.73)$$


where, $A_h(\mathbf{k})$ denotes the portability amplitude to emit a graviton of momentum \mathbf{k} (and definite helicity $h = \pm 2$). So the emission rate could be written as

$$d\Gamma_h(\mathbf{k}) = \frac{1}{T} \frac{d^3\mathbf{k}}{(2\pi)^3} \frac{1}{2|\mathbf{k}|} |A_h(\mathbf{k})|^2 \quad (3.74)$$

Now, considering all the possible diagrams contributing to $A_h(\mathbf{k})$ from the multipole action given in equation (3.46), yields

$$i\mathcal{A}_h(\mathbf{k}) = \frac{\text{diagram 1}}{I_{ij}} + \frac{\text{diagram 2}}{J_{ij}} + \frac{\text{diagram 3}}{I_{ijk}} + \dots \quad (3.75)$$

$$i\mathcal{A}_h(\mathbf{k}) = \frac{i}{4m_{Pl}} \epsilon_{ij}^*(\mathbf{k}, h) \left[\mathbf{k}^2 I^{ij}(k) + \frac{4}{3} |\mathbf{k}| \mathbf{k}^l \epsilon^{ikl} J^{jk}(k) - \frac{i}{3} \mathbf{k}^2 \mathbf{k}^l I^{ijl}(k) + \dots \right]. \quad (3.76)$$

Then we can sum over the helicities using the identity given in equation (107) in [40] and the power radiated could be written as⁴

$$\begin{aligned} P &= \int 2|\mathbf{k}| \sum_h d\Gamma_h(\mathbf{k}) \\ &= \frac{G_N}{\pi T} \int d|\mathbf{k}| \left[\frac{|\mathbf{k}|^6}{5} |I^{ij}(|\mathbf{k}|)|^2 + \frac{16|\mathbf{k}|^6}{45} |J^{ij}(|\mathbf{k}|)|^2 + \dots \right]. \end{aligned} \quad (3.77)$$

Converting the above equation into time domain, we get

$$P = \frac{G_N}{5} \left\langle \left(\frac{d^3}{dt^3} I^{ij}(t) \right)^2 \right\rangle + \frac{16G_N}{45} \left\langle \left(\frac{d^3}{dt^3} J^{ij}(t) \right)^2 \right\rangle + \dots \quad (3.78)$$

The original derivation of this result can be found in [40] in the context of NRGR, and agrees with the results derived by Kip Thorne in 1980 [41].

3.10 Radiation Reaction

In this section, we compute the real part of the diagrams contributing to the S_{EFT} in equation (3.47). This real part is expected result in the back reaction of the power radiated on the dynamics of the binary. One expects the parameters of the binary like its radius, total mass, etc. to change due to the emission of the gravitational waves converting the conservative dynamics of the binary into a dissipative one. If one naively starts to calculate the real part of the leading diagram given in figure 3.5a,

⁴The radiated power is proportional to the first time derivative of the monopole or the second time derivative of the dipole. But, the monopoles and the dipoles are conserved due to $\partial_\mu \mathcal{T}^{\mu\nu} = 0$ and hence do not contribute to the radiated power.

$$S_{EFT(\text{fig-3.5a})} = -\frac{G_N}{20} \int dt \frac{d}{dt} \left(\frac{d^2}{dt^2} I_{ij} \right)^2, \quad (3.79)$$

the contribution would be a total derivative and thus zero. This happened because of the In-Out formalism used to compute the correction. The review of the In-Out formalism, the problems with it, and the introduction to the correct formalism called the In-In formalism is developed in [44, 45]. We present the In-In formalism for NRGR and compute a non-zero correction responsible for the decaying of the orbits of the binary as given in [44] in the following subsections.

3.10.1 In-In Formalism - For NRGR

To obtain the generating function for NRGR, we need to double the radiation graviton field and the sources fields as well. For this, we need to introduce two types of auxiliary sources - $\mathbf{j}_{(1,2)}$ that couples to the trajectory of the binary $\mathbf{x}_{(1,2)}$ and $J_{(1,2)}^{\mu\nu}$ that couples to the radiation graviton $\bar{h}_{(1,2)}^{\mu\nu}$. The generating function for the NRGR in In-In formalism is then given by

$$e^{iW[\mathbf{j}_{k(1)}, \mathbf{j}_{k(2)}, J_{(1)}^{\mu\nu}, J_{(2)}^{\mu\nu}]} = \int D\mathbf{x}_{k(1)} D\mathbf{x}_{k(2)} D\bar{h}_{(1)}^{\mu\nu} D\bar{h}_{(2)}^{\mu\nu} \exp \left\{ iS_{NRGR}[\mathbf{x}_{k(1)}, \bar{h}_{(1)}^{\mu\nu}] - iS_{NRGR}[\mathbf{x}_{k(2)}, \bar{h}_{(2)}^{\mu\nu}] \right. \\ \left. + i \int dt (\mathbf{j}_{k(1)} \cdot \mathbf{x}_{k(1)} - \mathbf{j}_{k(2)} \cdot \mathbf{x}_{k(2)}) + i \int d^4x (J_{\mu\nu(1)} \bar{h}_{(1)}^{\mu\nu} - J_{\mu\nu(2)} \bar{h}_{(2)}^{\mu\nu}) \right\} \quad (3.80)$$

where the subscript 1 denotes fields propagating forward in time and 2 denotes propagating backward in time. The generating function for the radiation gravitons in the basis, $J_+ = (J_{(1)} + J_{(2)})$ and $J_- = (J_{(1)} - J_{(2)})$ can be written as

$$Z_0[J_{\pm}^{\mu\nu}] = \exp \left\{ \frac{-1}{2} \int d^4x \int d^4y J_a^{\mu\nu}(x) D_{\mu\nu\alpha\beta}^{ab}(x-y) J_b^{\alpha\beta}(y) \right\}. \quad (3.81)$$

The matrix of the propagator is given by

$$D_{\mu\nu\alpha\beta}^{ab}(x-x') = \begin{pmatrix} 0 & -iD_{\mu\nu\alpha\beta}^{adv} \\ -iD_{\mu\nu\alpha\beta}^{ret} & \frac{1}{2}D_{\mu\nu\alpha\beta}^H \end{pmatrix}. \quad (3.82)$$

where, $D_{\alpha\beta\gamma\delta}^H(x, x') = \langle \{ \bar{h}_{\alpha\beta}(x), \bar{h}_{\gamma\delta}(x') \} \rangle$. The equation of motion for the point particles and radiation gravitons could be found using

$$0 = \frac{\delta\Gamma}{\delta\langle \hat{\mathbf{x}}_{k-} \rangle} \Bigg|_{\mathbf{x}_{k-}=0, \mathbf{x}_{k+}=\mathbf{x}_k, \mathbf{j}_{k\pm}=J_{\pm}^{\mu\nu}=0} \quad (3.83)$$

$$\langle \bar{h}_{\mu\nu}(t, \mathbf{x}) \rangle = \frac{\delta e^{iW}}{\delta J_-^{\mu\nu}(t, \mathbf{x})} \Bigg|_{\mathbf{x}_{k-}=0, \mathbf{x}_{k+}=\mathbf{x}_k, \mathbf{j}_{k\pm}=J_{\pm}^{\mu\nu}=0} \quad (3.84)$$

respectively, where $\mathbf{x}_{k+} = (\mathbf{x}_{k(1)} + \mathbf{x}_{k(2)})$, $\mathbf{x}_{k-} = (\mathbf{x}_{k(1)} - \mathbf{x}_{k(2)})$ and similarly for \mathbf{j}_{\pm} . One should be using the above given equations to get a correct result while calculating quantities that have a causal dependence like power radiated or back reaction.

3.10.2 Calculating Radiation Reaction

We now try to compute the back reaction of the radiated power on the dynamics of the binary. For this, we use the above developed formalism to calculate the real part of the leading diagram contributing to back reaction at order Lv^5 ,

$$\begin{aligned} iS_{EFT(\text{fig-3.5a})}[\mathbf{x}_{K\pm}] &= \left(\frac{1}{2}\right) \left(\frac{i}{2m_{pl}}\right)^2 \int dt \int dt' Q_a^{ij}(t) \langle E_{ij}^a(t') E_{kl}^b(t') \rangle Q_b^{kl}(t') \\ &= -\frac{1}{80m_{pl}^2} \int dt \int dt' \left[-2iQ_-^{ij}(t) \frac{d^2}{dt^2} \frac{d^2}{dt'^2} D_{ret}(t-t', \mathbf{0}) Q_+^{ij}(t') \right. \\ &\quad \left. + \frac{1}{2} Q_-^{ij}(t) \frac{d^2}{dt^2} \frac{d^2}{dt'^2} D_H(t-t', \mathbf{0}) Q_-^{ij}(t') \right] \end{aligned} \quad (3.85)$$

where, the following expression for the propagator is used

$$\langle E_{ij}^a(t) E_{kl}^b(t') \rangle = \frac{1}{20} \left[\delta_{ik} \delta_{jl} + \delta_{ik} \delta_{jl} - \frac{2}{3} \delta_{ij} \delta_{kl} \right] \frac{d^2}{dt^2} \frac{d^2}{dt'^2} D^{ab}(t-t', \mathbf{0}). \quad (3.86)$$

Now using the leading order expression for the quadrupole moment given in the equation (3.58) and ignoring all the terms of $O(\mathbf{x}_-^2)$ ⁵ we get,

$$Q_-^{ij}(t) = \sum_K m_K \left\{ x_{K-}^i x_{K+}^j + x_{K+}^i x_{K-}^j - \frac{2}{3} \delta^{ij} \mathbf{x}_{K-} \cdot \mathbf{x}_{K+} \right\} \quad (3.87)$$

$$Q_+^{ij}(t) = \sum_K m_K \left\{ x_{K+}^i x_{K+}^j - \frac{1}{3} \delta^{ij} \mathbf{x}_{K+}^2 \right\} \quad (3.88)$$

where, $Q_-^{ij}(t) = Q_1^{ij}(t) - Q_2^{ij}(t)$ and $Q_+^{ij}(t) = \frac{1}{2}(Q_1^{ij}(t) + Q_2^{ij}(t))$. Substituting the above in equation (??) we get

$$iS_{EFT(\text{fig-3.5a})}[\{\mathbf{x}_{K\pm}\}] = -\frac{i}{80\pi m_{pl}^2} \int dt \sum_{K=1}^2 m_K x_{K-}^i(t) x_{K+}^j(t) \frac{d^5 Q_+^{ij}(t)}{dt^5} \quad (3.89)$$

which could not be transformed into a total derivative. This result was first derived in [44] using the formalism of NRGR, which agrees to the previously derived result by Kip Thorne in 1969 [46] and by William Burke in 1971 [47]. This gives us an acceleration after using equation (3.83) corresponding to the above given radiation reaction as

$$\mathbf{a}_{rr}^i(t) = -\frac{2G_n}{5} \mathbf{x}^j(t) I^{ij(5)}(t). \quad (3.90)$$

⁵One can drop such terms because these drop out while finding the dynamics of the binary using the equation (3.83).

Form this, using the results given in section 4 of [45], we get the energy balance equation as

$$\left\langle \frac{dM(t)}{dt} \right\rangle = \sum_a m_a \langle \mathbf{a}_{rr}^i(t) \mathbf{v}^i(t) \rangle = -\frac{G_n}{5} \langle I^{ij(3)}(t) I^{ij(3)}(t) \rangle \quad (3.91)$$

which exactly matches the amount of power radiated to infinity given in equation (3.78). Using the above defined techniques, one can now calculate the power radiated to infinity and its back-reaction on the dynamics of the binary up to desired PN order.

3.11 Dissipative Effects

In this section, we compute the effects of the dissipative sector of the internal structure of the compact object on their dynamics in the binary system as computed in [48]. Using the result of matching done in section 2.3, the $\text{Im} [F(\omega)]$ corresponding to response quadrupole moment of the dissipative sector is given by

$$\text{Im} [F(\omega)] = \frac{16}{45} G_N^5 m^6 \omega \quad (3.92)$$

Now once we have the relation between the $\text{Im} [F(\omega)]$ and the M_{pl} , we now compute the scaling of the leading order dissipative term as

$$\frac{1}{M_{pl}} \int d\tau Q_{ij} E^{ij}[H] \approx v^{13/2} \quad (3.93)$$

Following the matching procedure, one can easily find that this is the leading order contribution of the dissipative sector of the internal structure of the compact object to the effective point particle Lagrangian in the PN expansion. The vertex given in equation (3.93) contributes first to the effective action by the diagram given in figure 3.9 which scales as Lv^{13} .

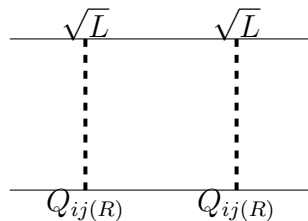


Figure 3.9: This diagram represents the leading order contribution of the dissipative internal structure of the compact objects to the effective action given in equation (3.9).

Thus the internal structure of the compact objects (response conservative sector) first contributes to the dynamics of the binary at 6.5PN. The power absorbed by the Fock space

of the response quadrupole moment is given by the imaginary part of the above diagram as

$$P_{abs} = \frac{16}{45} m_2^2 m_1^6 G_N^7 \left\langle \left(\frac{d}{dt} q_{ij(1)} \right)^2 \right\rangle + 1 \leftrightarrow 2 \quad (3.94)$$

where, $q_{ij}(t) = (\delta_{ij} - 3n_i n_j)/|r(t)|^3$. This result was first derived in [48] using the formalism of NRGR, and agrees to the previously derived result in [49, 50] in the limit $m_1 \ll m_2$. This is the power absorbed from the binding potential to the Fock space of the response quadrupole moment.

3.12 Higher-order Corrections

In this section, we briefly describe the effects of term S_{NL} in the equation (3.31) on the radiated power by the binary. This term leads us to the three-point and four-point vertices for radiation gravitons, where its scaling could be seen from the schematic form given by

$$\frac{1}{M_{pl}} \int d^4x \bar{h}^2 \partial^2 \bar{h} \approx \frac{v^2}{\sqrt{r}} \quad \text{and} \quad \frac{1}{M_{pl}^2} \int d^4x \bar{h}^3 \partial^2 \bar{h} \approx \frac{v^4}{r} . \quad (3.95)$$

We also have nonlinear vertices where n gravitons are emitted by the binary. We just mention such diagrams in this section, ignoring calculation of the exact corrections since these diagrams contribute to higher PN order than the usual diagram considered till now. The detail calculation corresponding to the these diagrams is given in [39]. Also, in this section, we only show the diagrams contributing to the power radiated, but one can combine these diagrams to get the contribution to the back reaction using the cutting rules given chapter 8 of [43].

3.12.1 Tail Effects

First, we look at the correction which is linear in the multipole moments. These correspond to the diagrams given in figure 3.10, where, adding a three-point vertex also needs a term of the form equation (3.40) and thus the total scales as v^3 . Similarly, adding a four-point vertex needs two terms of the form equation (3.40) and thus the total scales as v^6 . So we expand the power radiated in orders of $\eta = R_s/\lambda \approx v^3$ which is called as Post-Minkowskian expansion.

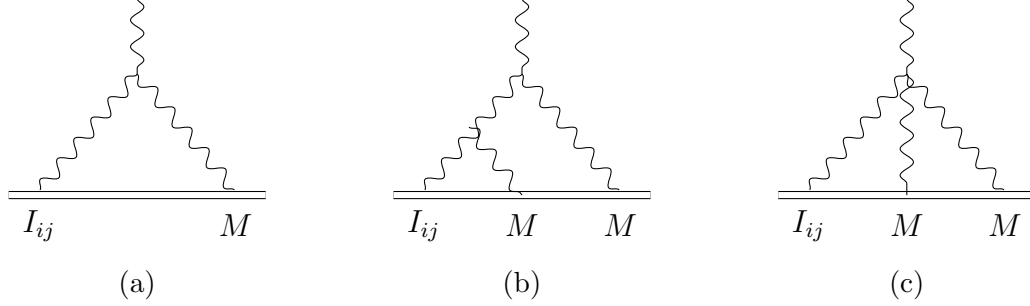


Figure 3.10: Examples of diagrams that contribute the power radiated and corresponds to the tails effects.

3.12.2 Non-linear Corrections

One way to obtain non-linear corrections to the power radiated is to replace a M by the l^{th} moment in a diagram contributing at order $\sqrt{Lv}(v)^n$ given in section 3.12.1. This will make new diagrams like the ones given in figure 3.11a, where, the l^{th} moment contribute at order $\sqrt{Lv}(v)^{n+l}$.

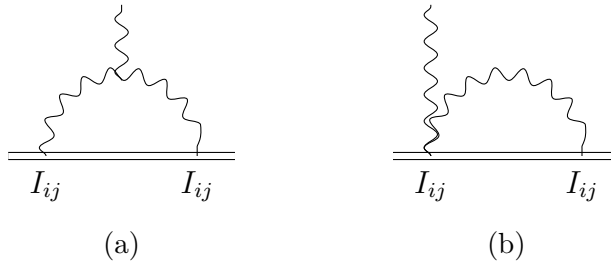


Figure 3.11: Examples of diagrams that contribute the power radiated and corresponds to the non-linear effects.

One can also have a vertex nonlinear in the radiation gravitons in a diagram that contributes to the power radiated. One can easily show that such non-linear vertices scale as η^n . For example, the nonlinear vertex in diagram given in figure 3.11b, where we have two gravitons coming out scales like η at the leading order. Whereas, the vertex with 3 gravitons coming out scale as $v^5\sqrt{v}/\sqrt{L}$, but it also needs an extra vertex at least of the form (3.40) which scales like \sqrt{Lv} . So the net scaling of the diagram increases by an order η^2 .

Chapter 4

Spinning Compact Objects

In this chapter, we try to model the spin of the constituents of the binary using the techniques developed by Rafael Porto in [4] in the context of Non-Relativistic General Relativity (NRGR). For this, we first describe the action that governs the dynamics of a spinning point particle on an arbitrary background. Then we describe the procedure to construct an Effective Field Theory (EFT) to describe the internal structure of the compact objects. Using two such spinning objects, we then study the effects of spin on the dynamics of the binary and extend the NRGR formalism developed in chapter 3 to include the additional degrees of freedom of spin. For this, we mention the power counting rules and Feynman rules for the action. We derive the effective potential for spinning particle up to 2PN and the contribution of spin to the EFT describing the internal structure of the point particle. To describe the effects of spin on emitted radiation to infinity by the binary, we find the contribution to spin on the EFT of multipole moments.

4.1 Action for a Spinning Point Particle

The equations governing the dynamics of the spinning particle on an arbitrary fixed curved background was given by Myron Mathisson and Achille Papapetrou equations [51, 52]. We first mention all the assumptions and derive the equation of motion for a spinning point particle called as Mathisson-Papapetrou equation. We then describe the extension of this formalism to include the dynamics of the background in linearized limit as given in [4].

4.1.1 Fixed Background

In this subsection, we follow the description of a spinning point particle given by A.J Hanson and T Regge in [53]. To model the spin, we add rotational degrees of freedom to the worldline of the point particle. These rotational degrees are encoded in the tetrads that connects the general Lorentz frame and the body-fixed frame of the rotating object.¹ The angular velocity of the rotating frame is given by

$$\sigma^{\mu\nu} = e_A^\mu \frac{de_B^\nu}{d\tau} \eta^{AB}. \quad (4.1)$$

¹We use the capital Latin indices to denote the body-fixed frame, small Latin indices to denote local Lorentz frames and Greek indices to denote general coordinate frame.

Now one can act Lorentz transformation on the general coordinate frame (Right action of the Lorentz group) as well as on the body fixed frame (Left action of the Lorentz group). We construct the Lagrangian for the spinning particles using the invariant under the action of the Lorentz transformation on the general coordinate frame (Right Invariant) because left transformation parameterizes the internal degree of the particle, but the right transformation are the symmetry of GR. These right invariants are given as

$$U_\mu U^\mu ; \quad \sigma_{\mu\nu} \sigma^{\mu\nu} ; \quad U_\mu \sigma^{\mu\nu} \sigma_{\nu\lambda} U^\lambda \quad \text{and} \quad \frac{1}{16} \sigma^{\mu\nu} \epsilon_{\mu\nu\lambda\rho} \sigma^\lambda . \quad (4.2)$$

In addition to this, we also have the re-parametrization invariance of the action for a point particle, which constraints the Lagrangian to be a homogeneous degree one function of the generalized velocities. One can easily show that the Hamiltonian for such system will be zero and thus the Lagrangian could be written as

$$L_{pp} = -P_\mu U^\mu - \frac{1}{2} S_{\mu\nu} \sigma^{\mu\nu} \quad (4.3)$$

where the conjugate momentum of the worldline coordinate x^μ and the tetrad e_A^μ is given by

$$P_\mu = \frac{\partial L_{pp}}{\partial U^\mu} \quad \text{and} \quad S_{\mu\nu} = 2 \frac{\partial L_{pp}}{\partial \sigma^{\mu\nu}} \quad (4.4)$$

respectively. One then observes that the spin tensor has more independent degrees of freedom than required to encode the spin vector. For this one has to add a gauge constraint² given by

$$S_{\mu\nu} P^\nu = 0. \quad (4.5)$$

The above equation physically constraints the center of mass of the object such that the axis of rotation has to pass through center of mass defined in the rest frame of the point particle.

Using the Lagrangian given in the equation (4.3) we can get the equation of motion for each coordinate for a fixed background. For this, we use the scheme used in [55]. We vary the worldline δx^μ by a small parameter ϵ such that the tetrads are parallelly transported to the new worldline. Similarly, the variation of the tetrad δe_A^μ is obtained by keeping the worldline fixed.

For the variation δe_A^μ ,

$$\begin{aligned} \frac{\delta L_{pp}}{\delta \epsilon} &= -\frac{1}{2} S_{\mu\nu} \frac{\delta \sigma^{\mu\nu}}{\delta \epsilon} \\ &= -\frac{1}{2} S_{\mu\nu} \frac{\delta}{\delta \epsilon} \left[e_A^\mu \frac{de_B^\nu}{d\tau} \eta^{AB} \right] \\ &= -\frac{1}{2} \left[-S_{\mu\nu} \frac{de_A^\mu}{d\tau} \eta^{AB} - \frac{d}{d\tau} (S_{\mu\nu}) e_A^\mu \eta^{AB} - S_{\mu\nu} \frac{de_A^\mu}{d\tau} \eta^{AB} \right] \frac{\delta e_B^\nu}{\delta \epsilon} \\ & \quad \frac{dS_{\mu\nu}}{d\tau} = [S_{\nu\beta} \sigma_\mu^\beta - S_{\mu\beta} \sigma_\nu^\beta] \end{aligned} \quad (4.6)$$

²More details about different spin gauges and their physical interpretation is given in [54].

For the variation δx^μ ,

$$\begin{aligned}
\frac{\delta L_{pp}}{\delta \epsilon} &= -P_\mu \frac{\delta U^\mu}{\delta \epsilon} - \frac{1}{2} S_{\mu\nu} \frac{\delta \sigma^{\mu\nu}}{\delta \epsilon} \\
&= -P_\mu \frac{d}{d\tau} \frac{\delta x^\mu}{\delta \epsilon} - \frac{1}{2} S_{\mu\nu} \frac{\delta}{\delta \epsilon} [e_A^\mu \frac{de_B^\nu}{d\tau} \eta^{AB}] \\
&= -\frac{dP_\mu}{d\tau} \frac{\delta x^\mu}{\delta \epsilon} - \frac{1}{2} S_{\mu\nu} \frac{\delta e_A^\mu}{\delta \epsilon} \frac{de_B^\nu}{d\tau} \eta^{AB} - \frac{1}{2} S_{\mu\nu} e_A^\mu \frac{\delta}{\delta \epsilon} \left[\frac{de_B^\nu}{d\tau} \right] \eta^{AB} \\
&= -\frac{dP_\mu}{d\tau} \frac{\delta x^\mu}{\delta \epsilon} - \frac{1}{2} S_{\mu\nu} e_A^\mu R^\nu_{\lambda\alpha\sigma} U^\sigma e_B^\lambda \frac{\delta x^\alpha}{\delta \epsilon} \eta^{AB} \\
&= \left[-\frac{dP_\alpha}{d\tau} - \frac{1}{2} S_{\mu\nu} e_A^\mu R^\nu_{\lambda\alpha\sigma} U^\sigma e_B^\lambda \eta^{AB} \right] \frac{\delta x^\alpha}{\delta \epsilon} \\
\frac{dP_\alpha}{d\tau} &= \frac{1}{2} S_{\mu\nu} R^{\mu\nu}_{\alpha\sigma} U^\sigma
\end{aligned} \tag{4.7}$$

The above-given equation in (4.6) and (4.7) are called as Mathisson-Papapetrou equations [51, 52]. These equations govern the dynamics of the spinning point particle, i.e. the position of the particle (3 components) and its spin vector (3 components).

4.1.2 Semi-classical Background

Now, we consider the spinning point particle on a semi-classical background. Their gravitational interaction is encoded in the gravitons ($h_{\mu\nu}$) given by

$$g_{\mu\nu} = \eta_{\mu\nu} + \frac{h_{\mu\nu}}{M_{pl}}. \tag{4.8}$$

Using the above-given decomposition and the relation given in equation (4.1), we can write the tetrad in a series expansion of $h_{\mu\nu}$ as

$$e_A^\mu = \delta_A^\mu + \frac{1}{2} \frac{h_A^\mu}{M_{pl}} - \frac{1}{8} \frac{h^\mu_\alpha h^\alpha_A}{M_{pl}} + \dots \tag{4.9}$$

One can also use the local Lorentz frame to simplify the calculation as it decomposes the $\sigma^{\mu\nu}$ as

$$\sigma^{\mu\nu} e_\mu^a e_\nu^b = \sigma^{ab} + \omega_\mu^{ab} U^\mu \tag{4.10}$$

where, the Ricci rotation coefficients are given by $\omega_\mu^{ab} = e_\nu^b \nabla_\mu e^{a\nu}$. The first term of RHS in the above equation gives us the kinetic term of the spin and the second term encodes the interaction of the spin with the graviton. Using the above equation, we can also decompose the action as

$$S_{pp} = \int ds \left[-P_\mu U^\mu - \frac{1}{2} S_{ab} \sigma^{ab} - \frac{1}{2} S_{ab} \omega_\mu^{ab} U^\mu \right] \tag{4.11}$$

Using the equation (4.9), one can expand the last term in the above action as

$$L_{\text{Spin}} = -\frac{1}{2} S_{\mu\nu} \partial^\mu h^\nu_\alpha U^\alpha - \frac{1}{4} S_{\mu\nu} h^\mu_\lambda \left[\partial_\alpha h^{\nu\lambda} + \partial^\mu h_\alpha^\lambda - \partial^\lambda h^\mu_\alpha \right] U^\alpha + \dots \tag{4.12}$$

which describes the interaction of the gravitons with the spin of the compact objects. This action given in equation (4.11) describes the complete action for the spinning point particle.

4.1.3 Contribution to the Internal structure

In this subsection, we repeat the procedure of constructing the EFT that encodes the internal structure of the compact object given in section 2.2. We again start with introducing the multipole moments and decomposing them into $\langle Q_{abc\dots k} \rangle_S$ - inherent multipole moments and $\langle Q_{abc\dots k} \rangle_R$ - the response multipole moments. But now, we do not have a spherically symmetric compact object, and thus, the inherent multipole moments are not zero. For example, the leading order the inherent quadrupole moment could be written using the allowed symmetries as

$$\langle Q_{ab} \rangle_S = \frac{C_{ES^2}}{2m} S^{ik} S_k^j. \quad (4.13)$$

The term contributing to the Lagrangian due to the above-given inherent quadrupole moment is given as

$$S_{ES^2} = i \frac{C_{ES^2}}{2m} \int d\tau d^4x \delta^4(x^\alpha - x_a^\alpha) \frac{E_{ij} S^{ia} S_a^j}{\sqrt{U^2}}. \quad (4.14)$$

Terms such as $\langle Q_{ab} \rangle_S$, acts as a classical background for the quantized perturbations $\langle Q_{ab} \rangle_R$. The inherent higher-order multipole moments could be added to the effective action, but we ignore all such corrections in this thesis. To simplify the calculations further, we assume the response of the multipole moments depends linearly on the incident gravitational waves. Thus the response quadrupole moments are given by

$$\langle Q_{ab} \rangle_R(\tau) = \frac{1}{2} \int d\tau' d^4x \delta^4(x - x(\tau')) G_{abij}^{ret}(\tau, \tau') E_{ij}(x) \quad (4.15)$$

where the causality is imposed using the retarded Green's function in the above equation, which is given as

$$G_{abij}^{ret}(\tau, \tau') = \langle [Q_R^{ab}(\tau), Q_R^{ij}(\tau')] \rangle \theta(\tau - \tau'). \quad (4.16)$$

In the frequency domain, the quadrupole propagator can be written as

$$iG_{abij}^{ret}(\omega) = Q_{abij} F(\omega) + S_{abij}(\omega) F_S(\omega) \quad (4.17)$$

where, the first term is already analyzed in section 2.2. Using the symmetries of the system, S_{abij} could be written as

$$S_{abij} = (\delta_{ai} S_{bj} + \delta_{aj} S_{bi} + \delta_{bj} S_{ai} + \delta_{bi} S_{aj})(1 + \alpha_S S^2) + O(S^3) \quad (4.18)$$

where, α_S is also an unknown coefficients and has to be determined using matching. Now, The tensor S_{abij} could be a function of ω as the spin tensor S_{ij} depends on ω . Similar to section 2.2, the real part of $G_{abij}^{ret}(\omega)$ is an even function of ω and thus describes the conservative sector whereas, the imaginary part of $G_{abij}^{ret}(\omega)$ is an odd function of ω and thus describes the dissipative sector. This could be easily generalized to the magnetic type and higher-order multipole moments.

Now we match the EFT to the full classical General Relativity (GR) to obtain the unknown Wilson coefficients. In the case of the conservative sector corresponding to the spin dependent part of the propagator, the combination of $S_{ijab}(\omega)F_S(\omega)$ should be even function of ω , which could also be thought of as even time derivatives acting on the E_{mn} in the effective action. The symmetries of the tensor S_{abij} make each term of the propagator anti-symmetric in two indices, which are contracted with the combination of E_{mn} symmetric in the corresponding two indices. Thus the spin does not contribute to the conservative sector of the effective action. For the dissipative sector, in the case of EFT, consider the diagram

$$\begin{aligned}
 \begin{array}{c} Q_{ij(R)} \\ \text{---} \\ Q_{ab(R)} \\ \text{---} \\ \text{wavy lines} \end{array} &= \frac{i}{8M_{pl}^2} \int d\tau e^{-i\omega\tau} \left(\omega^2 \epsilon_{ij}^* \epsilon_{ab} \left\langle Q_{ab}^{(E)}(0) Q_{ij}^{(E)}(\tau) \right\rangle \right. \\
 &\quad \left. + (\mathbf{k} \times \epsilon^*)_{ij} (\mathbf{k} \times \epsilon)_{ab} \left\langle Q_{ab}^{(B)}(0) Q_{ij}^{(B)}(\tau) \right\rangle \right) \quad (4.19)
 \end{aligned}$$

The imaginary part of the above diagram obtained by making the propagator of the response quadrupole moment on-shell. We use the plane wave with helicity $p = -2$ moving in the $\hat{\mathbf{z}}$ direction and decompose it in terms of spherical modes $Y_{lm}(\theta\phi)$. Using the dominant harmonic mode $l = 2$ and in the regime $R_S\omega \ll 1$ i.e. low frequency regime, we get the absorption cross-section

$$\sigma_{EFT}^{(abs)}(\omega) = \frac{\omega^3}{M_{pl}^2} \text{Im} \left[F(\omega) (1 + \alpha_S G_N^2 m^4 a_*^2) G_N m^2 a_* \right] \quad (4.20)$$

where $\mathbf{k} = \omega \hat{\mathbf{z}}$ and $\mathbf{S} \cdot \hat{\mathbf{z}} = a_* G_N m^2$. In the case of classical general relativity, the absorption cross-section for an axially symmetric object (Kerr spacetime) in the limit $\omega \ll m_l(a_*/4m)$, is given by [30]

$$\sigma_{GR}^{(abs)}(\omega) = \frac{4\pi}{45} R_S^5 \omega^3 (1 + 3a_*^2) a_* \quad (4.21)$$

Matching the above-given two results [56] we obtain

$$F_S(\omega) = \frac{4}{45} G_N^3 m^3 ; \quad \alpha_S = \frac{3}{m^4 G_N^2} \quad (4.22)$$

and the imaginary part of the quadrupole moment propagator comes from the contraction between polarization and spin tensors. This means that the time dependence in the RHS of equation (4.16) is entirely encoded in the spin of the point particle. The above result is exact for a Kerr black hole, and one has to perform the matching independently for a different object like neutron star using the graviton absorption cross-section in the corresponding metric.

4.2 Conservative Dynamics

In this section, we aim to calculate the contribution to the conservative binding potential of a binary due to the spin of the compact objects computed in [4]. For this, we consider the similar expansion parameters and field decomposition as given in section 3.1 and 3.2

respectively. The conservative sector the corresponds to $\bar{h}_{\mu\nu} = 0$. The effective action $W_{EFT}[x_p, S_{pp(a)}^{\mu\nu}(\sigma_a)]$ describing the conservative sector it is given by

$$e^{iW_{EFT}[x_{pp}^{(a)}, S_{pp(a)}^{\mu\nu}(\sigma_a)]} = \int D[H_{\mu\nu}] e^{iS_{EH}[H_{\mu\nu}] + iS_{int}[x_{pp}^{(a)}(\sigma_a), S_{pp(a)}^{\mu\nu}(\sigma_a), H_{\mu\nu}]} \quad (4.23)$$

where $S_{EH}[H_{\mu\nu}]$ describes the dynamics and self-interaction of the potential graviton and the S_{int} given by equation (2.12) and equation (4.50) that describes the dynamics of a point particle with internal structure and its interaction with potential gravitons. In the following subsections, we give a power counting for the spin degrees of freedom and the Feynman rules for the spin graviton interaction vertices.

4.2.1 Power counting

The gauge constraint given in equation (4.5) could be used to determine the relative scaling between $S_{\mu 0}$ and $S_{\mu i}$. Going to the rest frame of the particle the gauge constraint becomes

$$S_{\mu 0} + S_{\mu i} v^i = 0. \quad (4.24)$$

We can use the above relation to conclude that $S_{\mu 0}$ scales one order of velocity higher than $S_{\mu i}$. This constraint fixes the S_{0i} degrees of freedom and the spin angular momentum in given by $S^i = \epsilon^{ijk} S_{jk}$. This spin vector describes the angular momentum of the compact object and hence scales like

$$S \approx I\omega \approx mR_s^2 \frac{v_{rot}}{R_s} \approx mR_s v_{rot} \quad (4.25)$$

For maximally rotating compact objects ($v_{rot} \approx 1$), using the power counting developed in section 3.3.2, $S \approx Lv$. For co-rotating compact objects ($v_{rot}/R_s = v/r$), the $S \approx Lv^4$. As the rotation slows down, the scaling of the spin vector reduces, and the additional term with spin tensor becomes irrelevant. For the rest of the thesis, we assume the compact objects to rotate maximally.

4.2.2 Vertices

The scaling of the different terms emerging out of the linear term in gravitons given in the equation (4.11) are given as

$$\begin{aligned} \int ds S_{ij} \partial^i \frac{H_0^j}{M_{pl}} \approx \sqrt{L} v^2 \quad ; \quad \int ds S_{ij} \partial^i \frac{H_l^j}{M_{pl}} v^l \approx \sqrt{L} v^3 \quad ; \quad \int ds S_{i0} \partial^i \frac{H_0^0}{M_{pl}} \approx \sqrt{L} v^3 \quad ; \\ \int ds S_{i0} \partial^i \frac{H_j^0}{M_{pl}} v^j \approx \sqrt{L} v^4 \quad \text{and} \quad \int ds S_{i0} \partial^0 \frac{H_0^i}{M_{pl}} \approx \sqrt{L} v^4 \quad . \end{aligned} \quad (4.26)$$

The corresponding Feynman rules is given by

$$\begin{array}{c} \sqrt{Lv^2} \\ \text{---} \blacksquare \text{---} x_a(t) \\ \vdots \downarrow \mathbf{p} \\ H_0^0(t, \mathbf{p}) \end{array} \equiv - \sum_{a=1,2} \frac{i}{2M_{pl}} \int dt S_{ij} \partial^i e^{i\mathbf{p}\cdot\mathbf{x}_a(t)} ; \quad (4.27)$$

$$\begin{array}{c} \sqrt{Lv^3} \\ \text{---} \blacksquare \text{---} x_a(t) \\ \vdots \downarrow \mathbf{p} \\ H_l^j(t, \mathbf{p}) \end{array} + \begin{array}{c} \sqrt{Lv^3} \\ \text{---} \blacksquare \text{---} x_a(t) \\ \vdots \downarrow \mathbf{p} \\ H_0^0(t, \mathbf{p}) \end{array} \equiv - \sum_{a=1,2} \frac{i}{2M_{pl}} \int dt \left[S_{ij} \partial^i v^l + S_{i0} \partial^i \right] e^{i\mathbf{p}\cdot\mathbf{x}_a(t)} \quad \text{and} \quad (4.28)$$

$$\begin{array}{c} \sqrt{Lv^4} \\ \text{---} \blacksquare \text{---} x_a(t) \\ \vdots \downarrow \mathbf{p} \\ H_j^0(t, \mathbf{p}) \end{array} + \begin{array}{c} \sqrt{Lv^4} \\ \text{---} \blacksquare \text{---} x_a(t) \\ \vdots \downarrow \mathbf{p} \\ H_0^i(t, \mathbf{p}) \end{array} \equiv - \sum_{a=1,2} \frac{i}{2M_{pl}} \int dt \left[S_{i0} \partial^i v^l + S_{0j} \partial^0 \right] e^{i\mathbf{p}\cdot\mathbf{x}_a(t)} \quad (4.29)$$

respectively. The higher-order terms could be similarly found by expanding the equation (4.11). The scaling of the leading term in the EFT due to internal structure of the particle given in equation (4.50) is given by

$$\frac{C_{ES^2}}{m} \int d\tau \partial_i \partial_j \frac{H_{00}}{M_{pl}} S^{ia} S_a^j \approx C_{ES^2} \sqrt{Lv^4} \quad (4.30)$$

where we will see in section 4.4 that the C_{ES^2} does not scale and is a constant depending on the compact object. The above vertex corresponds to the following Feynman diagram

$$\begin{array}{c} \sqrt{Lv^4} \\ \text{---} \blacksquare \text{---} x_a(t) \\ \vdots \downarrow \mathbf{p} \\ H_{00}(t, \mathbf{p}) \end{array} \equiv - \sum_{a=1,2} \frac{iC_{ES^2}}{2m M_{pl}} \int d\tau \partial_i \partial_j S^{ia} S_a^j e^{i\mathbf{p}\cdot\mathbf{x}_a(t)} \quad (4.31)$$

In addition to the above-given vertices, we have vertices coming from the action of a point particle and Einstein-Hilbert action provided in section 3.3.3. All the higher-order terms in $H_{\mu\nu}$ and S_{muv} will scale with the higher power of v . In the next section, we aim to calculate the binding potential up to 2PN, and so, all such higher-order terms are ignored.

4.3 Calculating Potential

In this section, we compute the contribution of spin of the compact objects to the conservative effective action given in equation (4.23). We have obtained this action by integrating out potential gravitons and ignoring the radiation ones. Here also we only consider the connected diagrams and ignore all the diagrams that contain graviton loops. We also

ignore all the diagrams with graviton self-energy terms which could be made zero by the techniques of dimensional regularization.

The effect of spin on the conservative dynamics of the binary could be separated into three categories according to their origin from the Lagrangian given in equation (4.11) as,

1. Spin-Orbit terms - where the spin vertex from one particle couples to the worldline vertex of the other.
2. Spin-Spin terms - where the spin vertex from one particle couples to the spin vertex of the other.
3. Spin-squared and higher-order spin vertices - where the vertex due to internal structure of the point particle couples to either to the orbit of the spin vertex of the other particle.

We here only calculate the leading order potential due to each type of diagram. At order Lv^3 we have the leading order Spin-Orbit diagrams given in figure 4.1 and could be computed using the result in equation (B.3) of [33]. The corresponding Lagrangian is given by

$$L_{SO(1.5PN)} = -2G_N m_2 \left[(\hat{\mathbf{r}} \times \mathbf{v}_1) \cdot \mathbf{S}_1 - (\hat{\mathbf{r}} \times \mathbf{v}_2) \cdot \mathbf{S}_1 \right] + 1 \leftrightarrow 2 \quad (4.32)$$

At order Lv^4 , we have two different kinds of diagram given in figure 4.2, which could be computed using equation (B.4) of [33]. The figure 4.2a corresponds to the leading order Spin-Spin interaction given by the Lagrangian

$$L_{SS(2PN)} = \frac{G_N}{\mathbf{r}^3} \left[\mathbf{S}_1 \cdot \mathbf{S}_2 - 3(\mathbf{S}_1 \cdot \hat{\mathbf{r}})(\mathbf{S}_2 \cdot \hat{\mathbf{r}}) \right]. \quad (4.33)$$

The figure 4.2b corresponds to the leading order contribution of the internal structure of the spinning compact objects, and the corresponding Lagrangian is given by

$$L_{S^2(2PN)} = \frac{C_{ES^2} G_N}{\mathbf{r}^3} \left[\frac{m_2}{m_1} (\mathbf{S}_1^2 - 3(\mathbf{S}_1 \cdot \hat{\mathbf{r}})^2) + \frac{m_1}{m_2} (\mathbf{S}_2^2 - 3(\mathbf{S}_2 \cdot \hat{\mathbf{r}})^2) \right]. \quad (4.34)$$

These Lagrangians are a correction to the previously computed Lagrangians in section 3.4. The original derivation of these results can be found in [4] in the context of NRGR, and agrees with the previously derived results in [57, 58].



Figure 4.1: These diagrams contribute to order Lv^3 to the effective action in equation (4.23).



Figure 4.2: These diagrams contribute to order Lv^4 to the effective action in equation (4.23).

Now to find the equation of motion, we cannot directly use the Euler-Lagrange equations because of the Lagrangian is written in terms of x^μ , U^μ and $S^{\mu\nu}$. We have to first make a partial Legendre transformation to obtain a Routhian given by

$$-R = -\frac{1}{2}S_{ab}\sigma^{ab} - L_{pp} = P_\mu U^\mu + \frac{1}{2}S_{ab}\omega_\mu^{ab}U^\mu \quad (4.35)$$

from this we can calculate the equation of motion for spin using Hamiltonian equations and that for the worldline using Euler-Lagrange given by

$$\frac{dS_{ab}}{d\tau} = \{S_{ab}, R\} = 4S^{ca}\eta^{bd}\frac{\partial R}{\partial S^{cd}} \quad \text{and} \quad \frac{\delta}{\delta x^\mu} \int d\tau R = 0 \quad (4.36)$$

respectively. The higher-order terms could be found by using the techniques of temporal Kaluza-Klein parametrization of the metric suggested by Kol and Smolkin in [34]. This simplifies the three and higher point interaction vertices by replacing them with simple vertices but more in number. The 3PN and higher order calculations could be found in [59, 60, 61, 62, 63]. The public package EFTofPNG [38], which was created for high-precision computation in the EFT of PN Gravity, could also be used to carry the higher PN calculations.

4.4 Contribution to the Internal structure

In this section, we analyze the effects of the internal structure of the spinning compact object on their dynamics in the binary system. The Spin-squared term starts contributing to the effective action at 2PN for maximally rotating compact objects in compact binaries. This is very interesting to us because now one can comment about the internal structure of the compact object in the inspiral phase at 2PN as oppose to 5PN in a non-rotating case seen in section 3.5.

In the equation (4.13), the quadrupole moment of the compact object could be identified as

$$Q^{\mu\nu} = \frac{C_{ES^2}}{2m} S^{\mu\alpha} S_\alpha^\nu \quad (4.37)$$

With this identification, one can find the relation between the quadrupole moment and the angular momentum for different objects and fix the unknown coefficient C_{ES^2} . For Kerr spacetime the required relation is $Q = S^2/m$ as given in [41], which sets $C_{ES^2} = 1$. For neutron stars, the relation is $Q = aS^2/m$, where a is constant that depends on the mass of the neutron star and the equation of state. The value of a is determined in [64] using numerical techniques to be around 2 to 8 and thus $C_{ES^2} \approx 2 - 8$.

4.5 Dissipative Dynamics

Following the section 3.6, we here derive the effects of spin on the waveform of the radiated wave and power carried by it. The point particle Lagrangian that encodes the interaction of radiation gravitons, potential gravitons and the spin of the constituents is

$$\begin{aligned} L_{pp} = & -\frac{1}{2}S_{\mu\nu}\partial^\mu H^\nu_\alpha U^\alpha - \frac{1}{4}S_{\mu\nu}H^\mu_\lambda \left[\partial_\alpha H^{\nu\lambda} + \partial^\mu H_\alpha^\lambda - \partial^\lambda H^\mu_\alpha \right] U^\alpha + \dots \\ & -\frac{1}{2}S_{\mu\nu}\partial^\mu \bar{h}^\nu_\alpha U^\alpha - \frac{1}{4}S_{\mu\nu}\bar{h}^\mu_\lambda \left[\partial_\alpha H^{\nu\lambda} + \partial^\mu H_\alpha^\lambda - \partial^\lambda H^\mu_\alpha \right] U^\alpha + \dots \end{aligned} \quad (4.38)$$

where, the effects of first line give us the conservative dynamics computed in section 4.3, and the effects of second line are considered in this section. In the following subsection, we give the vertices corresponding to the interaction terms of spin, potential gravitons and radiation gravitons. Then we calculate the multipole moments for the binary defined in section 3.7. Using the computed multipole moments, we compute the effects of the spin on the emitted waveform and the radiated power.

4.5.1 Vertices

The scaling of the different terms emerging out of the linear term in gravitons given in the equation (4.11) are given as

$$\int ds S_{ij} \partial^i \frac{\bar{h}^j_0}{M_{pl}} \approx \sqrt{L} v^2 \quad ; \quad \int ds S_{ij} \partial^i \frac{\bar{h}^j_l}{M_{pl}} v^l \approx \sqrt{L} v^3 \quad \text{and} \quad \int ds S_{i0} \partial^i \frac{\bar{h}^0_0}{M_{pl}} \approx \sqrt{L} v^3 \quad . \quad (4.39)$$

The corresponding Feynman rules are given by

$$\begin{aligned} \text{---} \overset{\sqrt{L} v^2}{\blacksquare} \text{---} x_a(t) \\ \quad \quad \quad \downarrow \text{P} \\ \quad \quad \quad \bar{h}^j_0(t, \mathbf{p}) \end{aligned} \quad \equiv \quad - \sum_{a=1,2} \frac{i}{2M_{pl}} \int dt S_{ij} \partial^i e^{i\mathbf{p} \cdot \mathbf{x}_a(t)} \quad \text{and} \quad (4.40)$$

$$\begin{array}{c} \sqrt{Lv}^3 \\ \text{---} \blacksquare \text{---} x_a(t) \\ \vdots \downarrow \mathbf{p} \\ \bar{h}^j_l(t, \mathbf{p}) \end{array} + \begin{array}{c} \sqrt{Lv}^3 \\ \text{---} \blacksquare \text{---} x_a(t) \\ \vdots \downarrow \mathbf{p} \\ \bar{h}^0_0(t, \mathbf{p}) \end{array} \equiv - \sum_{a=1,2} \frac{i}{2M_{pl}} \int dt \left[S_{ij} \partial^i v^j + S_{i0} \partial^i \right] e^{i\mathbf{p} \cdot \mathbf{x}_a(t)} \quad (4.41)$$

respectively. The higher-order terms could be similarly found by expanding the equation (4.38).

4.5.2 Calculating Multipole Moments

Now we calculate the diagrams with one graviton in the final state, which contributes to the total $T_{\mu\nu}$ using the point particle action given in equation (3.31). Then we use the above-given relations between the multipole moments and the stress-energy tensor to obtain the exact expression for the moments for first few orders in v .



Figure 4.3: These diagrams yield the $\mathcal{T}^{\mu\nu}$.

The diagram that contributes to order $\sqrt{Lv}v^2$ is given in figure 4.3a. This corresponds to the stress-energy tensor,

$$\mathcal{T}^{0i}(t, \mathbf{k}) = \sum_{a=1,2} S^{ij} \mathbf{k}^j e^{-i\mathbf{p} \cdot \mathbf{x}_a(t)} \quad (4.42)$$

which leads to,

$$\mathbf{L}_i = \sum_a \mathbf{S}_i \quad ; \quad (4.43)$$

$$J^{ij} = \sum_a [\mathbf{S}^i \mathbf{x}^j + \delta^{ij} \mathbf{S} \cdot \mathbf{x}]_{\text{STF}} \quad ; \text{ and so on.} \quad (4.44)$$

where, the angular momentum of the binary gets a contribution from the angular momentum of the constituents. The diagram that contributes to order $\sqrt{Lv}v^3$ is given in figure 4.3b. This corresponds to the stress-energy tensor,

$$T^{00}(t, \mathbf{k}) = \sum_{a=1,2} S^{0i} \mathbf{k}^i e^{-i\mathbf{p}\cdot\mathbf{x}_a(t)} \quad (4.45)$$

$$\mathcal{T}^{ij}(t, \mathbf{k}) = \sum_{a=1,2} S^{il} \mathbf{v}^j \mathbf{k}^l e^{-i\mathbf{p}\cdot\mathbf{x}_a(t)} \quad (4.46)$$

which leads to,

$$\mathbf{X}^i = \sum m_a S_a^{0i} \quad ; \quad (4.47)$$

$$I^{ij} = \sum_a 2 \left[S^{0i} \mathbf{x}^j + (\mathbf{S} \times \mathbf{v})^i \mathbf{x}^j \right]_{\text{STF}} \quad ; \quad \text{and so on.} \quad (4.48)$$

where, the center of mass of the binary gets a contribution from the energy due to the angular momentum of constituents encoded in S_a^{0i} .

All the higher-order corrections to the multipole moments are ignored in this thesis and could be found in [65]. At order $\sqrt{Lv}(v)^n$, the first multipole moment M scales like $\sqrt{Lv}(v)^n$ and each l^{th} order moment scales like $\sqrt{Lv}(v)^{n+l}$. An important thing to notice is, the knowledge about the orbits of the binary is required to obtain any physical quantity using the multipole moments.

Now one can easily calculate the emitted waveform and the power radiated using the above given multipole moments in the equation (3.71) and equation (3.78) respectively. To calculate the radiation-reaction, we can use the above derived multipole moments instead of equation (3.87) and (3.88) in the section 3.10 to get a result similar to equation (3.89).

4.6 Dissipative Effects

In this section, we compute the effects of the dissipative sector of the internal structure of the compact object on their dynamics in the binary system as computed in [56]. Using the result of matching done in section 4.1.3, the $\text{Im}[F(\omega)]$ corresponding to response quadrupole moment of the dissipative sector is given by

$$\text{Im}[F_S(\omega)] = \frac{4}{45} G_N^3 m^3 \quad \text{and} \quad \alpha_S = \frac{3}{m^4 G_N^2}. \quad (4.49)$$

Once we have the relation between the $\text{Im}[F(\omega)]$ and the M_{pl} , we compute the scaling of the leading order dissipative term as

$$\frac{1}{M_{pl}} \int d\tau Q_{ij} E^{ij}[H] \approx v^5 \sqrt{(1 + 3a_*^2) a_*} \quad (4.50)$$

The vertex given in the above equation contributes first to the effective action by the diagram given in figure 4.4.

The power absorbed by the Fock space of the response quadrupole moment is given by

the imaginary part of the above diagram as

$$P_{abs} = -\frac{8}{5}m_2^2m_1^5G_N^6 \left\langle \frac{(\mathbf{r} \times \dot{\mathbf{r}}) \cdot \mathbf{S}}{r^8} (1 + 3a_\star^2)a_\star \right\rangle \quad (4.51)$$

This is the power absorbed from the binding potential to the Fock space of the response quadrupole moment. The original derivation of this result can be found in [56] in the context of NRGR, and agrees with the previously derived results in [50, 66].

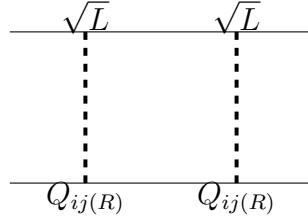


Figure 4.4: This diagram represents the leading order contribution to order $Lv^{10}(1 + 3a_\star^2)a_\star$ of the dissipative internal structure of the spinning compact objects to the effective action given in equation (4.23).

Chapter 5

Charged Compact Objects

In this chapter, we extend the NRGR described in chapter 3 to incorporate the effects of electromagnetic charge on the constituents of the binary. We incorporate the photon field in Non-Relativistic General Relativity (NRGR) by giving the field decomposition and power counting rules. Using these, we develop the Feynman rules to describe photon and graviton interactions with point particle worldline. We then find the corrections to the Einstein-Infeld-Hoffmann (EIH) Lagrangian due to the presence of the photon field and electromagnetic charge on the constituents of the binary.

5.1 Action for the Photon

The total action governing the dynamics of the binary is given by

$$S_{\text{Total}} = M_{pl}^2 \int d^4x \sqrt{-g} R + \int d^4x \sqrt{-g} \left[\frac{1}{4\mu_0} g^{\mu\alpha} g^{\nu\beta} F_{\mu\nu} F_{\alpha\beta} \right] + S_{\text{pp}}^{(a)} \quad (5.1)$$

where the first term is the Einstein-Hilbert action that governs the dynamics of the underlying spacetime denoted by S_{EH} with M_{pl} being the Planck's length. The second term governs the dynamics of the electromagnetic field and is denoted by S_{EM} where, $F_{\mu\nu} = \nabla_\mu A_\nu - \nabla_\nu A_\mu$ is the electromagnetic stress energy tensor minimally coupled to the background, A_μ is the corresponding photon field, and μ_0 is the magnetic permeability of vacuum. The term $S_{\text{pp}}^{(a)}$ is the action for each constituent of the binary (approximated as point particles) and contains their interaction with the electromagnetic field as well as the underlying spacetime. It is given by

$$S_{\text{pp}}^{(a)} = \int ds \left[-m_{(a)} \sqrt{g_{\mu\nu} U_{(a)}^\mu U_{(a)}^\nu} + q_{(a)} U_{(a)}^\mu A_\mu \right] + S_{\text{EFT}}^{(a)} \quad (5.2)$$

where $m_{(a)}$, $q_{(a)}$ and $U_{(a)}^\mu$ are the mass, electromagnetic charge and the four velocity of the a^{th} point particle respectively. The effective Lagrangian $S_{\text{EFT}}^{(a)}$ contains the effective operators and Wilson coefficients that encode the internal structure of the constituents of the binary. We will ignore this term in this analysis as its leading contribution to conservative sector for a spherically symmetric object starts at 2.5PN for acceleration induced multipole moments [67], 3PN for multipole moments describing the tidal effects due to external electromagnetic waves [48] and 5PN for multipole moments describing the tidal effects due to external gravitational waves [3].

5.2 Expansion Parameter

In addition to a expansion parameter (v/c and \hbar/L) given in section 3.1, we have another parameter when electromagnetic interactions are added to the theory,

$$\frac{\mu_0 q_1 q_2}{G_N m_1 m_2} = \epsilon. \quad (5.3)$$

In this thesis we consider three cases: first, $\epsilon \ll 1$ which describes the gravitational force being dominant with corrections from electromagnetic force. Here we have ϵ as another expansion parameter with v/c . Second is $\epsilon = 1$ which describes the system with both forces of equal magnitude and thus we dont have any other expansion parameter. Third is $1/\epsilon \ll 1$ which describes the electromagnetic force being dominant with corrections from gravitational force. Here we have $1/\epsilon$ as another expansion parameter with v/c .

5.3 Field Decomposition

The effective action S_{eff} that describes the dynamics of binary is obtained after integrating over the gravitons and photons given by

$$e^{iS_{eff}[x_{pp}^{(a)}(\sigma_a)]} = \int D[h_{\mu\nu}] D[A_\alpha] e^{iS_{EH}[g_{\mu\nu}] + iS_{EM}[A_\alpha, g_{\mu\nu}] + iS_{int}[x_{pp}^{(a)}(\sigma_a), g_{\mu\nu}, A_\alpha]} \quad (5.4)$$

where $x_{pp}^{(a)}(\sigma_a)$ is the position of the a^{th} point particle in the binary, and the integration is over the gauge fixed fields. As we are only interested in the long-distance physics at the scales of λ , we similar decomposition is done for the photon field to obtain long distance modes - radiation photons (\bar{A}_μ) and short distance modes - potential photons (\mathbf{A}_μ) as

$$A_\mu = \mathbf{A}_\mu + \bar{A}_\mu. \quad (5.5)$$

This decomposition is done according to [3] by identifying the modes by their scaling with respect to v and r . The long distance modes represent the emitted on-shell fields and its momentum scales as

$$(k_0, \mathbf{k}) \approx \left(\frac{v}{r}, \frac{v}{r}\right) \quad (5.6)$$

because k_0 is the frequency of the excitation and should scale like the inverse of period of the binary given by r/v and so does \mathbf{k} because these are on-shell. Whereas, the short distance modes are off-shell and its momentum scales as

$$(k_0, \mathbf{k}) \approx \left(\frac{v}{r}, \frac{1}{r}\right) \quad (5.7)$$

because the wave vector \mathbf{k} has the dimensions of the inverse length and the only parameter at this scale is the distance between the particles in the binary given by $1/r$ and k_0 is the frequency of the excitation and should scale like the inverse of period of the binary given by r/v .

5.4 Conservative Dynamics

For calculating the binding potential of the binary, we only consider the dynamics of the potential modes, its interactions with point particles and ignore the radiation modes from now on in this thesis. This describes the conservative dynamics of the binary given by the effective action $W_{eff}[x_p]$,

$$e^{iW_{eff}[x_{pp}^{(a)}]} = \int D[H_{\mu\nu}]D[\mathbf{A}_\alpha] e^{iS_{EH}[H_{\mu\nu}] + iS_{EM}[H_{\mu\nu}, \mathbf{A}_\alpha] + iS_{int}[x_{pp}^{(a)}(\sigma_a), H_{\mu\nu}, \mathbf{A}_\alpha]} . \quad (5.8)$$

In this section, we describe the technique of power counting and give all the essential Feynman rules for propagators and vertices. Using these Feynman rules, we calculate the leading order correction to the binding potential at 1PN in the next section.

5.4.1 Propagators

We consider the equation (5.1), where the quadratic term gives us the propagator and the higher order terms give us the nonlinear interaction vertices. All the calculations from now on are carried out in the Lorenz gauge for both gravitons and photons. Due to small velocities of the point particles, the momentum space propagators for gravitons and photons can be expanded in series as

$$\frac{1}{k^2} \approx \frac{-1}{\mathbf{k}^2} \left[1 + \frac{k_0^2}{\mathbf{k}^2} + \frac{k_0^4}{\mathbf{k}^4} + \dots \right] . \quad (5.9)$$

Using the above leading order term, at leading order, the Feynman rule for the propagator of the potential photons in momentum space is given by

$$\mathbf{A}_\mu(t_1, \mathbf{p}) \overset{\text{-----}}{\overrightarrow{\mathbf{p}}} \mathbf{A}_\nu(t_2, \mathbf{p}) \equiv \frac{-i\eta_{\mu\nu}}{\mathbf{p}^2} \delta(t_1 - t_2) \quad (5.10)$$

and higher orders of k_0^2/\mathbf{k}^2 are taken into account by the propagator correction given by equation (5.12).

5.4.2 Power counting

To arrange the terms in the Lagrangian in increasing order of expansion parameter, we need to have a manifest power counting in v . For this, we need to know the scaling behavior of the field and its derivatives. At the leading order, the propagator for potential modes scales as v/r^2 and so the potential photons scale as

$$\mathbf{A}_\alpha(x) \approx \frac{\sqrt{v}}{r} . \quad (5.11)$$

For the third kind of vertex, $S_{\text{pp}}^{(a)}$ action given in (5.2) can be expanded as

$$\begin{aligned} \sum_{a=1,2} \int ds \left[q_a \frac{dx^\mu}{ds} A_\mu \right] d^4x \delta^4(x^\mu - x_a^\mu(s)) = \\ - \sum_{a=1,2} q_a \int dt \left[\mathbf{A}_0 \sqrt{\mu_0} - \mathbf{v}^i \mathbf{A}_i \sqrt{\mu_0} \right]. \end{aligned} \quad (5.14)$$

The Feynman rules and the scaling of the linear term in photon field coupling to the point particle worldline has the following Feynman rules and scaling,

$$\begin{array}{c} \sqrt{L} \\ \vdots \\ \downarrow \mathbf{p} \\ \vdots \\ \mathbf{A}_0(t, \mathbf{p}) \end{array} \mathbf{x}_a(t) \quad \equiv \quad -iq_a \sqrt{\mu_0} \int dt e^{i\mathbf{p} \cdot \mathbf{x}_a(t)} \quad \text{and} \quad (5.15)$$

$$\begin{array}{c} \sqrt{L} v^2 \\ \vdots \\ \downarrow \mathbf{p} \\ \vdots \\ \mathbf{A}_i(t, \mathbf{p}) \end{array} \mathbf{x}_a(t) \quad \equiv \quad -iq_a \sqrt{\mu_0} \int dt \mathbf{v}_a^i e^{i\mathbf{p} \cdot \mathbf{x}_a(t)}. \quad (5.16)$$

The terms that contribute to a higher order of v are ignored here. In addition to the above-given vertices, we have vertices coming from the action of a point particle and Einstein-Hilbert action provided in section 3.3.3.

In all the above diagrams, the vertices have to be contracted with the propagator having the corresponding free indices. For example, vertex with \mathbf{v}^i or $\mathbf{v}^i \mathbf{v}^j$ has to be contracted with $P_{i0_}$ or $P_{ij_}$ respectively. If a vertex does not have a free index then it should be contracted with $P_{00_}$. The order of ϵ that each vertex contributes to is not shown in the above given Feynman rules. This is different for the case of $\epsilon \ll 1$ and $1/\epsilon \ll 1$, which could be easily seen by the scaling of M_{pl} and μ_0 with ϵ in each vertex for each case.

5.5 Calculating Binding Potential

In this section, we explicitly calculate the first few terms of the effective Lagrangian for the action given in equation (5.8). We have obtained this action by integrating out potential gravitons and photons and ignoring the radiation ones. Similar to the diagrams corresponding to gravitons, we only consider connected photon diagrams, internal lines correspond to potential photons, and we do not have external on-shell potential photons. We ignore all the diagrams that contain photon loops and self-energy terms.



Figure 5.1: The digrams that contribute to order Lv^0 .

The diagrams contributing at order Lv^0 (for arbitrary order of ϵ) are given in figure 5.1. The equation (B.3) of [33] is used to compute the integrals in corresponding to the diagrams. The corresponding Lagrangian is given by

$$L_{(Lv^0)} = \sum_{a=1,2} \frac{1}{2} m_a \mathbf{v}_a^2 + \frac{G_N m_1 m_2}{|\mathbf{r}|} - \frac{\mu_0 q_1 q_2}{4\pi |\mathbf{r}|} \quad (5.17)$$

where the first term represents the kinetic energy of the particle, the second is the Newtonian gravitational potential with $G_N = 1/(32\pi M_{pl}^2)$ being the Newton's constant and the third is the Coulomb potential.

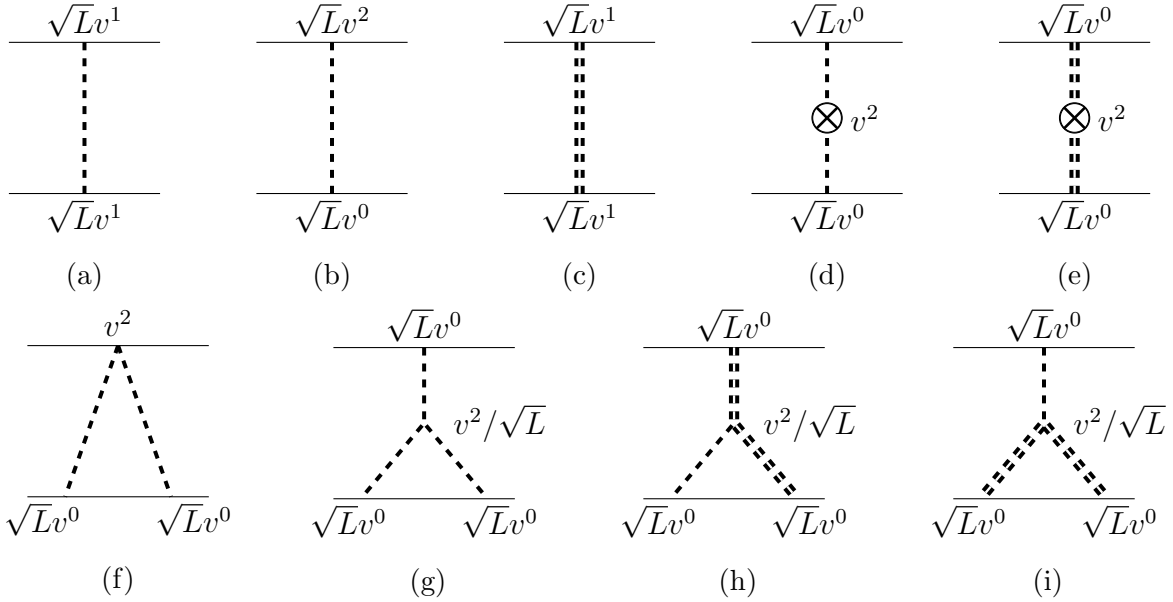


Figure 5.2: The digrams that contribute to order Lv^2 .

The diagrams contributing at order Lv^2 (for arbitrary order of ϵ) are given in figure 5.2. The diagrams 5.2a, 5.2b, 5.2c and 5.2f are straightforward to compute using equation (B.3) of [33]. For the diagram 5.2d and 5.2e we use equation (B.4) of [33] and for the diagram 5.2g,

5.2h and 5.2i, we use equations (B.4) of [33] and (A.34) in [33]. The results then correspond to the following Lagrangian

$$\begin{aligned}
L_{(Lv^2)} = & \sum_{a=1,2} \frac{1}{8} m_a \mathbf{v}_a^4 + \frac{G_N m_1 m_2}{2|\mathbf{r}|} \left[3(\mathbf{v}_1^2 + \mathbf{v}_2^2) - 7(\mathbf{v}_1 \cdot \mathbf{v}_2) - \frac{(\mathbf{v}_1 \cdot \mathbf{r})(\mathbf{v}_2 \cdot \mathbf{r})}{r^2} \right] \\
& - \frac{G_N^2 m_1 m_2 (m_1 + m_2)}{2\mathbf{r}^2} + \frac{\mu_0 q_1 q_2}{4\pi 2|\mathbf{r}|} \left[(\mathbf{v}_1 \cdot \mathbf{v}_2) + \frac{(\mathbf{v}_1 \cdot \mathbf{r})(\mathbf{v}_2 \cdot \mathbf{r})}{r^2} \right] \\
& + \frac{G_N \mu_0}{4\pi} \left[\frac{m_1 q_2 (q_1 + q_2) + m_2 q_1 (q_1 + q_2)}{2\mathbf{r}^2} \right]. \tag{5.18}
\end{aligned}$$

The first three terms of the above equation is the Einstein-Infeld-Hoffmann Lagrangian [5]. The next term is the correction to the EIH Lagrangian due to the charge on the constituents, which has also been derived using techniques of classical GR in [18]. The final term corresponds to the non-linear interaction between the gravitational and electromagnetic forces. This term has been newly calculated by the techniques detailed in this thesis.

The above results can now be analysed in the order of ϵ . For the case of $\epsilon \ll 1$ the hierarchy of diagrams is given in table 5.1. The corresponding terms in the Lagrangian could be easily recognized according to the power of μ_0 as it scales like ϵ . Similarly, for the case of $1/\epsilon \ll 1$ the hierarchy of diagrams is given in table 5.2 and the corresponding terms in the Lagrangian could be easily recognized according to the power of G_N because it scales like $1/\epsilon$. For the case of $\epsilon \approx 1$, the Lagrangian at order Lv^0 is given in equation (5.17) and at order Lv^2 is given in equation (5.18).

| | ϵ^0 | ϵ^1 | ... |
|----------|--------------|--------------|-----|
| v^0 | Figure 5.1a | Figure 5.1b | |
| v^2 | Figure 5.2a | Figure 5.2c | |
| | Figure 5.2b | Figure 5.2e | |
| | Figure 5.2d | Figure 5.2h | |
| | Figure 5.2f | Figure 5.2i | |
| | Figure 5.2g | | |
| \vdots | | | |

Table 5.1: The hierarchy of diagrams at different orders of v and ϵ for $\epsilon \ll 1$.

| | $1/\epsilon^0$ | $1/\epsilon^1$ | $1/\epsilon^2$ | \dots |
|----------|----------------------------|---|----------------------------|---------|
| v^0 | Figure 5.1b | Figure 5.1a | | |
| v^2 | Figure 5.2c Figure 5.2e | Figure 5.2a Figure 5.2b Figure 5.2d Figure 5.2h Figure 5.2i | Figure 5.2f Figure 5.2g | |
| \vdots | | | | |

Table 5.2: The hierarchy of diagrams at different orders of v and ϵ for $1/\epsilon \ll 1$.

Chapter 6

Discussion and Conclusion

This thesis is based on the study of the Effective Field Theory (EFT) approach developed by Walter Goldberger and Ira Rothstein in [3], as presented in chapters 2 and 3. This approach was primarily developed to tackle the two-body problem in General Relativity (GR) in the non-relativistic limit and hence called the Non-Relativistic General Relativity (NRGR). But several extension of this formalism, for example, to include the effects of the spin of the components [4] presented in chapter 4, were developed later. NRGR has an advantage over others because it decouples the highly non-linear nature of GR and its power counting rules allow us to determine the relevance of an operator at the level of action. In this approach, the perturbative calculations of a physical observable are conveniently performed by means of Feynman diagrams. The use of these diagrammatic techniques is quite natural when discussing an extension of this formalism to include different exotic effects. One such example is presented in [17], where the authors extend the NRGR formalism to include the effects of a light scalar degree of freedom, like the one possibly responsible for the accelerated expansion of the Universe.

In this thesis, we extend the NRGR formalism to include the effects of the electromagnetic charge on the constituents of the binary. A similar analysis was previously done in [18], but in a limit of charge of the binary constituents much more than their mass. In such a limit, one can only derive terms that are zeroth order in G_N . The techniques of NRGR allow us to follow through the analysis without assuming any such limit and thus gives a general result. The analysis is presented in chapter 5 and the result corresponds to equation (5.18), where we find an additional term over the previous results of [18] and [5]. We then prescribe the method to systematically study the correction due to the sub-dominant force in orders of $\epsilon \ll 1$ and $1/\epsilon \ll 1$ as given in table 5.1 and 5.2 respectively.

Several aspects of the formalism remain to be worked out. This analysis of studying the electromagnetic charge on the binary constituents can be extended further to higher PN orders using the techniques developed in [69] and to include the spin of the constituents of the binary using the analysis given in [4]. Here we have not discussed the effects of the radiation photons on the dynamics of the binary. Using the radiation photons, the leading order waveform and the radiated power by the binary in terms of its multipole expansion could be found in [40], but the higher-order effects due to the interaction of photon and graviton are yet to be analyzed. Such corrections have to be computed analogously to the analysis done for the radiation gravitons in [39]. Also, in our analysis of charged compact

objects so far, we have neglected the role of spins or higher rank tensors carried by the point particles. The photons do not interact with the spin directly in the point particle action except in the EFT describing the internal structure of the point particle. The EFT describing the internal structure of a charged compact objects contains highly non-trivial interaction terms of the gravitons, photons and the spin and thus deserves a careful analysis.

Bibliography

- [1] B. P. Abbott et al. Observation of Gravitational Waves from a Binary Black Hole Merger. *Phys. Rev. Lett.*, 116(6):061102, 2016.
- [2] B. P. Abbott et al. GW170817: Observation of Gravitational Waves from a Binary Neutron Star Inspiral. *Phys. Rev. Lett.*, 119(16):161101, 2017.
- [3] Walter D. Goldberger and Ira Z. Rothstein. An Effective field theory of gravity for extended objects. *Phys. Rev.*, D73:104029, 2006.
- [4] Rafael A. Porto. Post-Newtonian corrections to the motion of spinning bodies in NRGR. *Phys. Rev.*, D73:104031, 2006.
- [5] Albert Einstein, L. Infeld, and B. Hoffmann. The Gravitational equations and the problem of motion. *Annals Math.*, 39:65–100, 1938.
- [6] Bala R. Iyer. Experiments driving theory: Gravitational wave detection and the two body problem in general relativity. *Journal of Physics: Conference Series*, 716:012010, may 2016.
- [7] Albert Einstein. Näherungsweise Integration der Feldgleichungen der Gravitation. *Sitzungsberichte der Königlich Preußischen Akademie der Wissenschaften (Berlin)*, pages 688–696, January 1916.
- [8] Albert Einstein. Über Gravitationswellen. *Sitzungsberichte der Königlich Preußischen Akademie der Wissenschaften (Berlin)*, pages 154–167, January 1918.
- [9] R. A. Hulse and J. H. Taylor. Discovery of a pulsar in a binary system. , 195:L51–L53, January 1975.
- [10] Luc Blanchet. Gravitational Radiation from Post-Newtonian Sources and Inspiralling Compact Binaries. *Living Rev. Rel.*, 17:2, 2014.
- [11] A. Buonanno and T. Damour. Effective one-body approach to general relativistic two-body dynamics. *Phys. Rev.*, D59:084006, 1999.
- [12] Frans Pretorius. Evolution of binary black hole spacetimes. *Phys. Rev. Lett.*, 95:121101, 2005.
- [13] C. V. Vishveshwara. Scattering of Gravitational Radiation by a Schwarzschild Black-hole. *Nature*, 227:936–938, 1970.

- [14] C. V. Vishveshwara. Stability of the schwarzschild metric. *Phys. Rev. D*, 1:2870–2879, May 1970.
- [15] Alexandre Le Tiec. The Overlap of Numerical Relativity, Perturbation Theory and Post-Newtonian Theory in the Binary Black Hole Problem. *Int. J. Mod. Phys.*, D23(10):1430022, 2014.
- [16] Luc Blanchet. Analyzing Gravitational Waves with General Relativity. *Comptes Rendus Physique*, 20:507–520, 2019.
- [17] Adrien Kuntz, Federico Piazza, and Filippo Vernizzi. Effective field theory for gravitational radiation in scalar-tensor gravity. *JCAP*, 1905(05):052, 2019.
- [18] M. V. Gorbatenko. Obtaining equations of motion for charged particles in the $(v/c)^3$ -approximation by the einstein-infeld-hoffmann method. *Theoretical and Mathematical Physics*, 142(1):138–152, Jan 2005.
- [19] Alexey A. Petrov and Andrew E. Blechman. *Effective Field Theories*. WSP, 2016.
- [20] Aneesh V. Manohar. Introduction to Effective Field Theories. In *Les Houches summer school: EFT in Particle Physics and Cosmology Les Houches, Chamonix Valley, France, July 3-28, 2017*, 2018.
- [21] Thomas Appelquist and J. Carazzone. Infrared singularities and massive fields. *Phys. Rev. D*, 11:2856–2861, May 1975.
- [22] Steven Weinberg. Phenomenological Lagrangians. *Physica*, A96(1-2):327–340, 1979.
- [23] Sean M. Carroll. *Spacetime and Geometry: An Introduction to General Relativity*. Cambridge University Press, 2019.
- [24] John F. Donoghue. Introduction to the effective field theory description of gravity. In *Advanced School on Effective Theories Almunecar, Spain, June 25-July 1, 1995*, 1995.
- [25] John F. Donoghue, Mikhail M. Ivanov, and Andrey Shkerin. EPFL Lectures on General Relativity as a Quantum Field Theory. 2017.
- [26] Eric Poisson, Adam Pound, and Ian Vega. The Motion of point particles in curved spacetime. *Living Rev. Rel.*, 14:7, 2011.
- [27] Rafael A. Porto. The effective field theorist’s approach to gravitational dynamics. *Phys. Rept.*, 633:1–104, 2016.
- [28] Barak Kol and Michael Smolkin. Black hole stereotyping: Induced gravito-static polarization. *JHEP*, 02:010, 2012.
- [29] Sayan Chakrabarti, T erence Delsate, and Jan Steinhoff. New perspectives on neutron star and black hole spectroscopy and dynamic tides. 2013.

- [30] Don N. Page. Particle emission rates from a black hole: Massless particles from an uncharged, nonrotating hole. *Phys. Rev. D*, 13:198–206, Jan 1976.
- [31] M. Beneke and Vladimir A. Smirnov. Asymptotic expansion of Feynman integrals near threshold. *Nucl. Phys.*, B522:321–344, 1998.
- [32] Bernd Jantzen. Foundation and generalization of the expansion by regions. *JHEP*, 12:076, 2011.
- [33] Vitor Cardoso, Oscar J. C. Dias, and Pau Figueras. Gravitational radiation in $d \geq 4$ from effective field theory. *Phys. Rev.*, D78:105010, 2008.
- [34] Barak Kol and Michael Smolkin. Classical Effective Field Theory and Caged Black Holes. *Phys. Rev.*, D77:064033, 2008.
- [35] James B. Gilmore and Andreas Ross. Effective field theory calculation of second post-Newtonian binary dynamics. *Phys. Rev.*, D78:124021, 2008.
- [36] Stefano Foffa and Riccardo Sturani. Effective field theory calculation of conservative binary dynamics at third post-Newtonian order. *Phys. Rev.*, D84:044031, 2011.
- [37] Stefano Foffa and Riccardo Sturani. Dynamics of the gravitational two-body problem at fourth post-Newtonian order and at quadratic order in the Newton constant. *Phys. Rev.*, D87(6):064011, 2013.
- [38] Michele Levi and Jan Steinhoff. EFTofPNG: A package for high precision computation with the Effective Field Theory of Post-Newtonian Gravity. *Class. Quant. Grav.*, 34(24):244001, 2017.
- [39] Walter D. Goldberger and Andreas Ross. Gravitational radiative corrections from effective field theory. *Phys. Rev.*, D81:124015, 2010.
- [40] Andreas Ross. Multipole expansion at the level of the action. *Phys. Rev.*, D85:125033, 2012.
- [41] Kip S. Thorne. Multipole expansions of gravitational radiation. *Rev. Mod. Phys.*, 52:299–339, Apr 1980.
- [42] Matthew D. Schwartz. *Quantum Field Theory and the Standard Model*. Cambridge University Press, 2014.
- [43] M. J. G. Veltman. Diagrammatica: The Path to Feynman rules. *Cambridge Lect. Notes Phys.*, 4:1–284, 1994.
- [44] Chad R. Galley and Manuel Tiglio. Radiation reaction and gravitational waves in the effective field theory approach. *Phys. Rev.*, D79:124027, 2009.

- [45] Chad R. Galley, David Tsang, and Leo C. Stein. The principle of stationary nonconservative action for classical mechanics and field theories. 2014.
- [46] Kip S. Thorne. Nonradial Pulsation of General-Relativistic Stellar Models.IV. The Weakfield Limit. , 158:997, December 1969.
- [47] W. L. Burke. Gravitational radiation damping of slowly moving systems calculated using matched asymptotic expansions. *Journal of Mathematical Physics*, 12:401–418, January 1971.
- [48] Walter D. Goldberger and Ira Z. Rothstein. Dissipative effects in the worldline approach to black hole dynamics. *Phys. Rev.*, D73:104030, 2006.
- [49] Eric Poisson and Misao Sasaki. Gravitational radiation from a particle in circular orbit around a black hole. v. black-hole absorption and tail corrections. *Phys. Rev. D*, 51:5753–5767, May 1995.
- [50] Hideyuki Tagoshi, Shuhei Mano, and Eiichi Takasugi. PostNewtonian expansion of gravitational waves from a particle in circular orbits around a rotating black hole: Effects of black hole absorption. *Prog. Theor. Phys.*, 98:829–850, 1997.
- [51] Myron Mathisson. Neue mechanik materieller systemes. *Acta Phys. Polon.*, 6:163–2900, 1937.
- [52] Achille Papapetrou. Spinning test particles in general relativity. 1. *Proc. Roy. Soc. Lond.*, A209:248–258, 1951.
- [53] A.J Hanson and T Regge. The relativistic spherical top. *Annals of Physics*, 87(2):498 – 566, 1974.
- [54] Jan Steinhoff. Spin gauge symmetry in the action principle for classical relativistic particles. 2015.
- [55] Israel W Bailey, I. Lagrangian dynamics of spinning particles and polarized media in general relativity. *Commun.Math. Phys.*, 42:65–82, 1975.
- [56] Rafael A. Porto. Absorption effects due to spin in the worldline approach to black hole dynamics. *Phys. Rev.*, D77:064026, 2008.
- [57] B. M. Barker and R. F. O’Connell. Gravitational two-body problem with arbitrary masses, spins, and quadrupole moments. *Phys. Rev. D*, 12:329–335, Jul 1975.
- [58] B. M. Barker and R. F. O’Connell. Derivation of the equations of motion of a gyroscope from the quantum theory of gravitation. *Phys. Rev. D*, 2:1428–1435, Oct 1970.
- [59] Rafael A. Porto and Ira Z. Rothstein. The Hyperfine Einstein-Infeld-Hoffmann potential. *Phys. Rev. Lett.*, 97:021101, 2006.

- [60] Rafael A. Porto and Ira Z. Rothstein. Spin(1)Spin(2) Effects in the Motion of Inspiralling Compact Binaries at Third Order in the Post-Newtonian Expansion. *Phys. Rev.*, D78:044012, 2008. [Erratum: *Phys. Rev.*D81,029904(2010)].
- [61] Rafael A Porto and Ira Z. Rothstein. Next to Leading Order Spin(1)Spin(1) Effects in the Motion of Inspiralling Compact Binaries. *Phys. Rev.*, D78:044013, 2008. [Erratum: *Phys. Rev.*D81,029905(2010)].
- [62] Rafael A. Porto. Next to leading order spin-orbit effects in the motion of inspiralling compact binaries. *Class. Quant. Grav.*, 27:205001, 2010.
- [63] Michele Levi and Jan Steinhoff. Complete conservative dynamics for inspiralling compact binaries with spins at fourth post-Newtonian order. 2016.
- [64] William G. Laarakkers and Eric Poisson. Quadrupole moments of rotating neutron stars. *Astrophys. J.*, 512:282–287, 1999.
- [65] Rafael A. Porto, Andreas Ross, and Ira Z. Rothstein. Spin induced multipole moments for the gravitational wave flux from binary inspirals to third Post-Newtonian order. *JCAP*, 1103:009, 2011.
- [66] Eric Poisson. Absorption of mass and angular momentum by a black hole: Time-domain formalisms for gravitational perturbations, and the small-hole / slow-motion approximation. *Phys. Rev.*, D70:084044, 2004.
- [67] Chad R. Galley, Adam K. Leibovich, and Ira Z. Rothstein. Finite size corrections to the radiation reaction force in classical electrodynamics. *Phys. Rev. Lett.*, 105:094802, 2010.
- [68] N. E. J. Bjerrum-Bohr. Leading quantum gravitational corrections to scalar QED. *Phys. Rev.*, D66:084023, 2002.
- [69] Barak Kol and Michael Smolkin. Non-Relativistic Gravitation: From Newton to Einstein and Back. *Class. Quant. Grav.*, 25:145011, 2008.